CAPITAL UNIVERSITY OF SCIENCE AND TECHNOLOGY, ISLAMABAD

Scattering Through Cylindrical Waveguide Involving Lined Chamber

by

Sumaira Shahzadi

A thesis submitted in partial fulfillment for the degree of Master of Philosophy

in the

Faculty of Computing
Department of Mathematics

2019

CERTIFICATE OF APPROVAL

Scattering Through Cylindrical Waveguide Involving Lined Chamber

by

Sumaira Shahzadi

(MMT163015)

THESIS EXAMINING COMMITTEE

S. No.	Examiner	Name	Organization
(a)	External Examiner	Dr. Muhammad Ayub	QAU, Islamabad
(b)	Internal Examiner	Dr. Abdul Rahman Kashif	CUST, Islamabad
(c)	Supervisor	Dr. Muhammad Afzal	CUST, Islamabad

Dr. Muhammad Afzal
Thesis Supervisor
September, 2019

Dr. Muhammad Sagheer
Head
Dept. of Mathematics
September, 2019

Dr. Muhammad Abdul Qadir
Dean
Faculty of Computing
September, 2019

Author's Declaration

I Sumaira Shahzadi hereby state that my M.Phil thesis titled "**Scattering Through Cylindrical Waveguide Involving Linned Chamber**" is my own work and has not been submitted previously by me for taking any degree from Capital University of Science and Technology, Islamabad or anywhere else in the country/abroad.

At any time if my statement is found to be incorrect even after my graduation, the University has the right to withdraw my M.Phil Degree.

(Sumaira Shahzadi)
Registration No: MMT163015

Plagiarism Undertaking

I solemnly declare that research work presented in this thesis titled "**Scattering Through Cylindrical Waveguide Involving Linned Chamber**" is solely my research work with no significant contribution from any other person. Small contribution/help wherever taken has been dully acknowledged and that complete thesis has been written by me.

I understand the zero tolerance policy of the HEC and Capital University of Science and Technology towards plagiarism. Therefore, I as an author of the above titled thesis declare that no portion of my thesis has been plagiarized and any material used as reference is properly referred/cited.

I undertake that if I am found guilty of any formal plagiarism in the above titled thesis even after award of M.Phil Degree, the University reserves the right to withdraw/revoke my M.Phil degree and that HEC and the University have the right to publish my name on the HEC/University website on which names of students are placed who submitted plagiarized work.

(Sumaira Shahzadi)
Registration No: MMT163015

Acknowledgements

All praise is due to Allah, the Lord of the Worlds, who keeps us on the right path. I also yield witness that Prophet Muhammad(PBUH) is the last messenger of Allah whose life is a perfect model for whole mankind till the day of judgment. Allah also gave me health to continue my research and job together. I could not do anything without the help of Allah. First of all, I would like to thank my honorable adviser **Dr. Muhammad Afzal** for his continuous sincere support of my M.Phil study and related research. His patience, motivation and immense knowledge gave me right path in research. He supported me with his kind guidance all the time while enhancing the difficult thesis . Besides of my adviser, I would also like to thank the rest faculty of mathematics department **Dr. Muhammad Sagheer**, **Dr. Abdul Rehman Kashif**, **Dr. Rashid Ali** and **Dr. Shafqat Hussain** for their encouragement and insightful comments to widen my knowledge. They also enabled me to research in different fields of study. I could not fulfill my research without their precious support. I would not forget my fellows who had worked together and spent precious time in valuable discussion with me before deadlines. I would also thank senior students who helped me in difficult times. Last but not the least, I would thank to my father, husband, brothers, sisters and roommate friends for their spiritually support while writing the thesis.

(Sumaira Shahzadi)

Registration No: MMT163015

Abstract

The current thesis addresses a class of problems arising in the modeling of scattering of acoustic waves in ducts or channels having abrupt geometric changes with varying bounding surfaces. The main aim is to analyze the acoustic scattering in cylindrical expansion chamber containing waveguide together with inclusion of the flanges at interfaces. The inside walls of the chamber are coated with fibrous and perforated materials. The envisaged boundary value problems have been solved by using Mode-Matching technique. The transmission loss against frequency is analyzed with respect to the geometrical configuration and properties of dissipative material. The results show that variation in properties of absorbing material and change of geometric configuration significantly affect the scattering behavior.

Contents

List of Figures

Chapter 1

Introduction and Literature Survey

Acoustics is a branch of physics that deals with the study of pressure fluctuations in gasses, solids and liquids, such as vibrations. In prehistoric eras, acoustics played an important role in controlling sound in stadium, worship places and concert halls etc. But in recent era, the scope of acoustics is not limited to noise controlling issues and has application in almost all areas of science. It has been divided into different branches including medical acoustics, architectural acoustics, physical engineering acoustics and musical acoustics etc.

The applications of acoustics can be found in noise reduction problems that include: (i) Architectural noise issues; noise which produced in duct of heating and ventilation system, (ii) Noise issues in aerodynamic; propagation of noise in wind tunnels, (iii) In road transportation; exhaust noise from internal combustion engine and (iv) Construction and industrial noise; machinery, factories and building sites. Noise usually propagates in ducts or pipes.

The designs of such ducts or pipes play an important role in noise reduction. Since these are the main sources of energy transmission from one point to another point.

1.1 Literature Review

The reduction of noise pollution is very important now a days in our society. It is imparting very adverse and destructive effects on human as well as animals health. There is immensely need to study new structure which may helpful in reducing the harmful effects of such vibrating systems.

During the *6th* century BC, Pythagoras, who built up arithmetic in Greek culture, also considered vibrating strings and musical sounds. He found that by separating the length of a vibrating string into ratio of length the musical intervals can be created [1]. The traveling of sound in the form of waves explained by Vinci, 1500. In 1635, Gassendi determined the speed of sound utilizing firearms and accepting that the light of the flash is transmitted quickly. His value turned out to be $478m/s$.

Gassendi also noticed that the speed of sound did not rely upon the pitch of the sound, in contrary to the perspective on Aristotle, who had thought that high notes are transmitted quicker than low notes. Later in 1640, Mersenne measured the speed of sound first time in air which is $450m/s$ [2]. He also discovered his famous laws of strings. In 1650, Borelli and Viviani got an estimation of $350m/s$ for the speed of sound [3]. Likewise Bianconi, demonstrated that the speed of sound in air increases with temperature [4].

In 1660 Boyle proved that a medium is required for the traveling of sound. Newton provided the basis of physical acoustics and discovered the wave velocity relation in solids. Bernoulli in mid of *17th* century discussed vibration of a string with reference to frequency. At the end of *17th* and the start of *18th* century, Chladni analyzed the vibrations produced by sound. In the *19th* century, Tyndall worked over transmission of sound in atmosphere and combination of musical tones. Tyndall saw that longitudinal vibration was generated by rubbing a bar.

Tyndall got a waveform of musical sound. He noticed the effects of fog and water in different climate conditions on the transmission of sound. In *20th* century, Sabine [5] who is generally known as father of architectural acoustics, made quantitative measurement of sound in room and formed the acoustical theaters.

The higher order modes studied by Lee [6] generated in the expansion chamber having rigid type wall conditions. Here we will consider the scattering and dissipating of acoustic waves in cylindrical waveguides utilizing Mode-Matching techniques. Such problems are usually governed by Helmholtzs or Laplace type differential equations together with boundary conditions of Drichlet, Nuemann or Robin types.

Various analytical and numerical methods have been developed so far to discussed different physical problems, for instance [7]-[14]. Rawlin [15], Buyukaksoy et al, [16] and Ayub et al [17]-[18] utilized Wiener-Hopf (WH) approach to discuss the wave scattering in bifurcated and trifurcated waveguides. The present study is related to the acoustic scattering and dissipation in cylindrical waveguide.

The scattering of sound waves and cavity resonances due to sudden cross-sectional changes of guiding structure is discussed in [19] by Peat. The use of absorbing lining to reduce unwanted noise in circular waveguide is discussed in [20].

The scattering of sound in the presence of flanged inclusion in cylindrical waveguide is discussed in [21] and in rectangular waveguide [22]-[23]. Damir and Buyukaksoy [24] analyzed the reflection and transmission in a cylindrical waveguide with lining muffler. They used WH technique to find the solution of their problems. In the present thesis we have considered a similar duct configuration as is discussed in [24] and then has solved it by using Mode-Matching approach with different bounding properties.

The Mode-Matching technique is well known and has already been used in [25]-[30] to discuss different scattering problems. Here we have discussed the acoustic lining in cylindrical duct in the presence of flange inclusion. In this thesis, two different designs of such ducts or channels are discussed in Chapter *3* and Chapter *4*, respectively. The basic terminology and related historical background is given in Chapter *1*. The concluding remarks are given in Chapter *5*.

Chapter 2

Preliminaries

Acoustic is basically related to the study of sound. The word of acoustic is derived from the Greek word akouein which means "to hear". First time Greeks discussed the sound in terms of science. Initially Sauver used the word "acoustics" for the study of sound in the scientific way in 1701. Acoustics deals the generation, transmission and reception of vibrations; such as sound infrasound or ultrasound. The other sub disciplines are, environmental acoustics, architectural acoustics, bio acoustics and musical acoustics. It has great influence on many other branches of science as well [33]. Some concept related to this thesis work are explained in following sections.

2.1 Waves

In any medium the appearance of waves show the disturbance in that medium. The wave propagates and carries energy from one point of the medium to another. The characteristics of wave depends upon the nature of the medium, e.g, the wave length of water waves depends upon the depth of water. Sound waves, magnetic waves, elastic waves and cosmic waves are types of the waves produced in different mediums.

2.2 Waveguides

Waveguides are the structures that guide waves, as water waves, sound waves or electromagnetic waves. A hollow metal pipe is the common waveguide for the radio waves of high frequency. The slab and fiber or channel waveguides confine energy in one and two dimensions.

2.3 Acoustic Waves

Acoustic waves (also known as sound waves) are the type of longitudinal waves that propagate by means of adiabatic compression and decompression. Longitudinal waves are the waves that have the same direction of vibration as the direction in which they travel. Important quantities for describing acoustic waves are sound pressure, particle velocity, particle displacement and sound intensity. Acoustic waves travel with the speed that depends on the medium they are passing through.

2.4 Acoustic Wave Equation

The acoustic propagation in certain medium can be described mathematically in term of equations, known as acoustic wave equation. This equation can be derived from the physical laws of motion and equation of state. The derivation is explained in next subsections.

2.4.1 Conservation of Mass

The conservation of mass equation is related to the net flow of mass per unit volume per uni time to the instantaneous rate of change of mass density that is [34]

$$\frac{\partial \rho}{\partial t} + \bigtriangledown.(\rho \mathbf{u}) = 0, \tag{2.1}$$

where, ρ is instantaneous mass density and $\mathbf{u}$ is the fluid particle velocity vector. The equation (2.1) is also known as equation of continuity.

2.4.2 Conservation of Momentum

The conservation of momentum states the net flow of momentum per volume per unit time to the forces acting on it, that is [34]

$$\frac{\partial(\rho\overline{\mathbf{u}})}{\partial t} = - \bigtriangledown .(\rho\overline{\mathbf{u}})\overline{\mathbf{u}} - \bigtriangledown p + \rho\mathbf{g}, \tag{2.2}$$

where, p is the pressure, $\mathbf{g}$ is gravitational acceleration, $\bigtriangledown p$ denotes the exerting force and $\rho\mathbf{g}$ shows the body force. From above equation,

$$\frac{\partial(\rho\overline{\mathbf{u}})}{\partial t} + \bigtriangledown.(\rho\overline{\mathbf{u}})\overline{\mathbf{u}} = - \bigtriangledown p + \rho\mathbf{g}, \tag{2.3}$$

which implies

$$\left(\frac{\partial\rho}{\partial t} + \bigtriangledown.(\rho\overline{\mathbf{u}})\right)\overline{u} = \rho\left(\frac{\partial}{\partial t} + \overline{\mathbf{u}}.\bigtriangledown\right)\overline{\mathbf{u}} = - \bigtriangledown p + \rho\mathbf{g}. \tag{2.4}$$

On using the continuity condition, we may write

$$\rho\frac{D\overline{\mathbf{u}}}{Dt} = - \bigtriangledown p + \rho\mathbf{g}, \tag{2.5}$$

where $D/Dt = \partial/\partial t + \overline{\mathbf{u}}.\bigtriangledown$ is the total time derivative known as Stokes total time derivative [40] including first term to be time derivative and second term the convective term.

2.4.3 Equation of State

The thermodynamic behaviour of the fluid can be expressed in term of an equation known as equation of state i.e,

$$p = \rho r T, \tag{2.6}$$

where, p is the pressure in Pascal (Pa), T is the temperature in Kelvin (K) and r is the specific gas constant. A gas enclosed in a vessel having walls which are thermally conductive, the perfect gas isotherm can be written as

$$\frac{p}{p_0} = \frac{\rho}{\rho_0}, \tag{2.7}$$

where ρ_0 and p_0 are the static density and pressure respectively. When no heat loss or gained by the system then perfect adiabatic is

$$\frac{p}{p_0} = (\frac{\rho}{\rho_0})^{\gamma}, \tag{2.8}$$

where, γ is the ratio of specific heat at constant pressure C_p to the specific heat at constant volume i.e, $\gamma = C_p/C_v$. The condensation s, that yields change in density for given ambient fluid is define as

$$s = \frac{\rho - \rho_0}{\rho_0}. \tag{2.9}$$

With the aid of equation (2.9) the expression (2.7) can be written as,

$$\frac{p}{p_0} = (1+s)^{\gamma}, \tag{2.10}$$

which leads to

$$p = p_0 \left\{ 1 + \gamma s \frac{\gamma(\gamma-1)}{2!} s^2 + ... \right\}. \tag{2.11}$$

For linear relationship

$$p - p_0 \approx \gamma p_0 s + O(s^2). \tag{2.12}$$

The relationship between density fluctuation and pressure can also be written by using Taylor's expansion as

$$p = p_0 (\frac{\partial p}{\partial \rho})_{\rho=\rho_0} (\rho - \rho_0) + ..., \tag{2.13}$$

or

$$p - p_0 \approx \rho_0 (\frac{\partial p}{\partial \rho})_{\rho=-\rho_0} \frac{\rho - \rho_0}{\rho_0}, \tag{2.14}$$

or

$$p - p_0 \approx \rho_0 (\frac{\partial p}{\partial \rho})_{\rho-\rho_0} s + O(s^2). \tag{2.15}$$

By comparing equation (2.12) and (2.15) we get

$$\gamma = \frac{\beta}{\rho}, \tag{2.16}$$

where, $\beta = (\partial p/\partial \rho)_{\rho-\rho_0}$ is the adiabatic Bulk modulus. The expression (2.15) can also be written as by neglecting the higher order terms,

$$p = \beta s. \tag{2.17}$$

2.4.4 Linearized Acoustic Wave Equation

Consider the linearized continuity equation, for $s \ll 1$, with respect to spartial coordinates

$$\frac{\partial s}{\partial t} + \bigtriangledown.(\rho \overline{\mathbf{u}}) = 0. \tag{2.18}$$

Like wise linearized momentum equation in the absence of body forces,

$$\rho_0 \frac{\partial(\overline{\mathbf{u}})}{\partial t} = - \bigtriangledown p, \tag{2.19}$$

where, $\mid \overline{\mathbf{u}}. \bigtriangledown \overline{\mathbf{u}} \mid \ll \partial \overline{\mathbf{u}}/\partial t$ is neglected. By taking the divergence on both sides of (2.19) we get

$$\frac{\partial}{\partial t}(\bigtriangledown.\overline{\overline{\mathbf{u}}}) = -\frac{1}{\rho_0} \bigtriangledown^2 p. \tag{2.20}$$

Differentiate the (2.18) with respect to t we found

$$\frac{\partial^2 s}{\partial t^2} = -\frac{\partial}{\partial t}(\bigtriangledown.\overline{\mathbf{u}}). \tag{2.21}$$

From (2.20)and (2.21) we obtain,

$$\frac{\partial^2 s}{\partial t^2} = \frac{1}{\rho_0} \bigtriangledown^2 p. \tag{2.22}$$

On using (2.17) we get

$$\bigtriangledown^2 p = \frac{1}{c^2}\frac{\partial^2 p}{\partial t^2}, \tag{2.23}$$

where,

$$c = (\beta/\rho_0)^{1/2}, \tag{2.24}$$

gives the speed of sound in fluid of density ρ, having bulk modulus β.

2.5 Helmholtz Equation

On assuming the harmonic time dependence of pressure such as $p = Pe^{-i\omega t}$, the resulting equation from (2.23) gives

$$\bigtriangledown^2 P^2 + k^2 P = 0, \tag{2.25}$$

where $k = \omega/c$ is wave number in which ω is the angular frequency. The equation (2.25) is known as the Helmholtz's equation. Note that for rectangular coordinate

$$\bigtriangledown^2 = \frac{\partial^2}{\partial x^2} + \frac{\partial^2}{\partial y^2} + \frac{\partial^2}{\partial z^2},$$

and for cylindrical coordinates

$$\bigtriangledown^2 = \frac{\partial^2}{\partial r^2} + \frac{1}{r}\frac{\partial}{\partial r} + \frac{1}{r^2}\frac{\partial^2}{\partial \theta^2} + \frac{\partial^2}{\partial z^2}.$$

Thus in cylindrical coordinates the Helmholtz's equation becomes

$$\left\{\frac{\partial^2}{\partial r^2} + \frac{1}{r}\frac{\partial}{\partial r} + \frac{1}{r^2}\frac{\partial^2}{\partial r^2} + \frac{\partial^2}{\partial z^2} + k^2\right\}\phi(r, z) = 0. \tag{2.26}$$

2.6 Mode Matching Technique

Several analytical techniques have been developed to analyze the reflection, transmission and absorption of waves in waveguides. The choice of such techniques is

subjected to material and geometrical properties of the guiding structures as well as the governing system of the physical problem. One of the most frequently employed methods for the problems containing structural discontinuities and different distribution of impedances along the surfaces is Mode-Matching (MM) technique. This technique is based on the determination of field potentials in segments of guiding structure. These expansions involve unknown amplitudes. The matching of pressures and velocities at interfaces converts the differential system into linear algebraic systems. These systems are truncated and solved for the unknown amplitudes.

The applications of physical problems that are amenable by using MM technique are found in automobile industry, heating ventilation and air conditioning systems HVAC of buildings and engineering structures. The key component in HVAC or automobile industry is a duct like structure. This structure transport vibrational energy to the environment which is sometime termed as noise. Thus the designs of such components that help to minimize noise are significant.

Sometime such designs involve several geometric variations together with different material properties inside of the structures. The solution of such governing boundary value problems found against the physical problem of interest is not always easy to calculate. However the MM technique which is relatively an easy approach provides an interesting way forward to find the solution of such problems. Some of such solutions are explained in next Chapter *3* and *4*.

Chapter 3

Scattering through Lined Cylindrical Waveguide

In this chapter, we discuss two problems relating to the acoustic scattering in cylindrical ducts or channels. These problems are the extended form of the work done by Pullen [36]-[37].

Pullen discussed similar geometrical configurations containing rigid (Dirichlet) type boundary conditions. He used the Mode-Matching technique to determine the solution of his problem. Here the envisaged work is reviewed with impedance type boundary conditions. Such conditions are mathematically categorized as Robin or mixed type boundary conditions.

First problem comprises a semi-infinite cylindrical duct having a plane piston at the finite end, while the second problem contains infinite cylindrical waveguide including two semi-infinite duct sections. In later case, the finite end of these semi-infinite duct regions are joined together by means of vertical step discontinuities.

The mathematical modeling of these boundary value problems (BVPs) their solutions and graphical results are explained in next two sections.

3.1 Acoustic Scattering through a Single Lined Duct

Consider a semi-infinite cylindrical duct of radius $\overline{b}$ stretched along $\overline{z}$-direction in dimensional cylindrical coordinates system $(\overline{r}, \overline{\theta}, \overline{z})$, where over bars used here and henceforth stand for the dimensional setting of coordinates. The inside of the duct is filled with compressible fluid of density ρ and sound speed c. The physical configuration of the duct is as shown in the Figure.

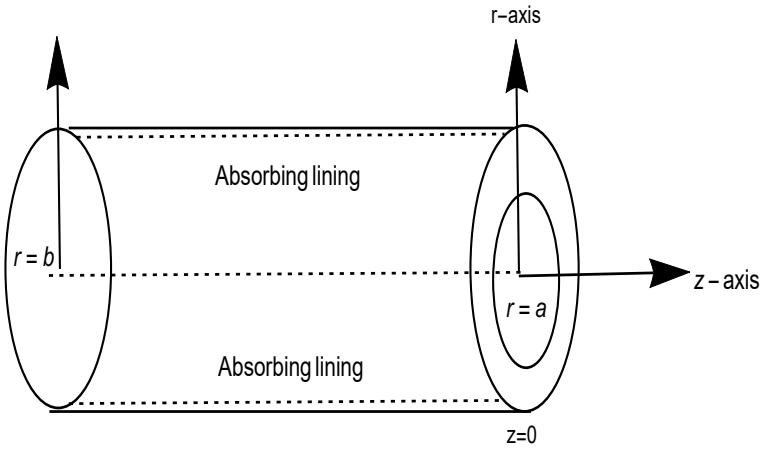

FIGURE 3.1: The geometry of duct.

The inside wall of the cylindrical duct comprises porous lining of absorbing material whereas, outside of it is set into *vacuo*. In a book by Morse and Ingard [38], the impedance of acoustic absorbing lining $\overline{Z}$ is defined by $\overline{Z} = \overline{p}/\overline{\mathbf{n}}.\overline{\mathbf{u}}$, where $\overline{p}$ and $\overline{\mathbf{u}}$ are the dimensional pressure and dimensional velocity respectively. Here the quantity $\overline{\mathbf{n}}$ denotes the normal unit vector directed into the lining. Let we

assume $\overline{\Phi}(\overline{r}, \overline{\theta}, \overline{z})$ the dimensional scalar field potential, then dimensional pressure and velocity are given as

$$\overline{p} = -\rho \frac{\partial \overline{\Phi}}{\partial t}, \tag{3.1}$$

and

$$\overline{\mathbf{u}} = \overline{\nabla}\ \overline{\phi}. \tag{3.2}$$

The boundary condition for absorbent surface can be given as

$$\overline{\mathbf{n}}.\overline{\nabla}\ \overline{\Phi} + \beta c^{-1} \frac{\partial \overline{\Phi}}{\partial t} = 0. \tag{3.3}$$

The quantity $\beta = \rho c Z^{-1}$ is specific admittance of the lining material. At $\overline{z} = \overline{0}$, there lies a plane piston in the annular disc which can move with dimensional velocity $\overline{U}_0$. The acoustic propagation in the duct given by acoustic wave equation [34]

$$\left\{ \frac{\partial^2}{\partial \overline{r}} + \frac{1}{\overline{r}} \frac{\partial}{\partial \overline{r}} + \frac{1}{\overline{r}^2} \frac{\partial^2}{\partial \overline{\theta^2}} + \frac{\partial^2}{\partial \overline{z}^2} \right\} \overline{\Phi} = \frac{1}{c^2} \frac{\partial^2 \overline{\Phi}}{\partial \overline{t}^2}. \tag{3.4}$$

On assuming the harmonic time dependence $e^{-i\omega \overline{t}}$, where ω is the radian frequency, the governing equation is Helmholtz's equation i.e,

$$\left\{ \frac{\partial^2}{\partial \overline{r}^2} + \frac{1}{\overline{r}} \frac{\partial}{\partial \overline{r}} + \frac{\partial^2}{\partial \overline{z}^2} + k^2 \right\} \overline{\psi}(\overline{r}, \overline{z}) = 0, \quad \overline{z} < \overline{0}, \quad \overline{0} \leq r \leq \overline{b}, \tag{3.5}$$

where,

$$\overline{\Phi}(\overline{r}, \overline{z}, \overline{t}) = e^{-i\omega t} \overline{\psi}(\overline{r}, \overline{z}),$$

in which $\overline{\psi}(\overline{r}, \overline{z})$ is the dimensional time independent field potential. We non-dimensionalize the BVP with respect to length scale k^{-1} and time scale ω^{-1} under the transformations

$$k\overline{r} = r \quad k\overline{z} = z \quad t = \omega \overline{t}, \tag{3.6}$$

and

$$\overline{\psi}(\overline{r}, \overline{z}) = \frac{\omega}{k^2} \psi(r, z) \tag{3.7}$$

where $\psi(r,z)$ be the non-dimensional velocity potential. By using these transformations, we may write,

$$\frac{\partial\overline{\psi}}{\partial\overline{r}}=\frac{\omega}{k}\frac{\partial\psi}{\partial r},\quad \frac{\partial^2\overline{\psi}}{\partial\overline{r}^2}=\omega\frac{\partial^2\psi}{\partial r^2},\quad \frac{\partial^2\overline{\psi}}{\partial\overline{z}^2}=\omega\frac{\partial^2\psi}{\partial z^2}. \tag{3.8}$$

Now with the aid of (3.6), (3.7) and (3.8) the equations (3.1), (3.3) and (3.5) can be given in dimensionless form as:

- Non-dimensional acoustic pressure

$$p=\frac{i\omega^2\rho}{k^2}\psi(r,z). \tag{3.9}$$

- Non-dimensional acoustic velocity

$$u=\frac{\omega}{k}\frac{\partial\psi}{\partial r}(r,z). \tag{3.10}$$

- Non-dimensional absorbing boundary condition,

$$\psi(r,z)+i\beta^{-1}\frac{\partial\psi}{\partial r}(r,z)=0,\quad r=b,z<0. \tag{3.11}$$

- Non-dimensional acoustic wave equation,

$$\left\{\frac{\partial^2}{\partial r^2}+\frac{1}{r}\frac{\partial}{\partial r}+\frac{\partial^2}{\partial z^2}+1\right\}\psi(r,z)=0,\quad z<0,\quad 0\le r\le b. \tag{3.12}$$

At $z=0$, the plane piston can be defined in non-dimensional form by

$$\frac{\partial\psi}{\partial z}=\begin{cases}U_0, & 0\le r\le a\\ 0, & a\le r\le b\end{cases}. \tag{3.13}$$

Here we have used $\overline{U}_0=cU_0$, where U_0 is the non-dimensional velocity. We solve this BVP by using MM technique. First we determine the eigen expansion of propagating modes in duct region by using the separation of variable technique, thus, we write

$$\psi(r,z)=R(r)Z(z). \tag{3.14}$$

On using (3.14) into (3.12), we get

$$\frac{R''}{R} + \frac{1}{r}\frac{R'}{R} + 1 = -\frac{Z''}{Z} = \eta^2. \tag{3.15}$$

From (3.15), after solving the differential equation for $Z(z)$, we found

$$Z(z) = Ae^{-i\eta z} + Be^{i\eta z}. \tag{3.16}$$

Note that the equation (3.16) yields the propagation of modes in positive and negative direction. Also from equation (3.15), we may write,

$$r^2R'' + rR' + r^2\tau^2R = 0, \tag{3.17}$$

which is Bessel differential equation, where $\tau = \sqrt{1-\eta^2}$ (see Abramowitz and Stegun [39]. The solution of this equation can be given as,

$$R(r) = CJ_0(\tau r) + DN_0(\tau r), \tag{3.18}$$

where $J_0(.)$ and $N_0(.)$ are the Bessel function of first and second kind respectively. Note that when $r \to 0$ the Bessel function of second kind becomes undefined therefore, we chose $D = 0$ for bounded solution hence,

$$R(r) = J_0(\tau r). \tag{3.19}$$

Now using (3.19) into (3.11) we found,

$$J_0(\tau b) + i\beta^{-1}J_0'(\tau b) = 0. \tag{3.20}$$

To calculate the derivatives of Bessel function we use the formula given in Abramovitz and stagun [39], that is,

$$\left(\frac{1}{z}\frac{d}{dz}\right)^k \{z^\nu J_\nu(z)\} = z^{\nu-k}J_{\nu-k}(z), \quad k = 0, 1, 2... \ . \tag{3.21}$$

Thus we may write (3.20) as,

$$J_0(\tau b) - i\beta^{-1}\tau J_1(\tau b) = 0, \tag{3.22}$$

which is characteristic equation for non-trivial solution. This characteristic equation can be solved numerically to get the eigenvalues of τ. There are infinite many values for which (3.22) holds thus, we may write eigenvalues as τ_n, and eigenfunction as $R_n(r) = J_0(\tau_n r)$ where $n = 0, 1, 2, ...\infty$. Hence,

$$\psi_n(r, z) = A_n R_n(r) e^{-i\eta_n z}, \tag{3.23}$$

yields the expression for n^{th} propagating mode in both positive and negative z-direction. Note that the coefficients A_n and B_n are the amplitudes of n^{th} modes propagating towards positive and negative z-direction, respectively. From superposition principle, the total field potential can be given by,

$$\psi(r, z) = \sum_{n=0}^{\infty} \psi_n(r, z). \tag{3.24}$$

Moreover, $R_n(r) \quad n = 0, 1, 2, ...$ subject to the eigen values τ_n are orthogonal in nature and satisfy the appropriate orthogonality relation, which is developed in aformensioned section.

3.1.1 Orthogonality Relation

To develop the orthogonality relation (OR) for eigenfunction $R_n = J_0(\tau_n r)$, $n = 0, 1, 2, ...$, we rewrite (3.17) and (3.20) as,

$$R_n^{''}(r) + \frac{1}{r} R_n^{'}(r) = -\tau_n^2 R_n(r), \quad 0 \leq r \leq b, \tag{3.25}$$

and

$$R_n(b) + i\beta^{-1} R_n^{'}(b) = 0. \tag{3.26}$$

We multiply (3.26) with $R_m(b)$ to get,

$$R_n(b)R_m(b) + i\beta^{-1}R_n^{'}(b)R_m(b) = 0. \tag{3.27}$$

By interchanging n by m, we found,

$$R_m(b)R_n(b) + i\beta^{-1}R_m^{'}(b)R_n(b) = 0. \tag{3.28}$$

On subtracting (3.28) from (3.27), we found,

$$R_m^{'}(b)R_n(b) + R_n^{'}(b)R_m(b) = 0, \tag{3.29}$$

which may be written as,

$$\left[r\left(R_m^{'}(r)R_n(r) + R_n^{'}(r)R_m(r)\right)\right]_{r=0}^{r=b} = 0. \tag{3.30}$$

Now on taking integration over r from $0 \leq r \leq b$, we obtain,

$$\int_0^b \frac{d}{dr}\left[r\left(R_m^{'}(r)R_n(r) + R_n^{'}(r)R_m(r)\right)\right]dr = 0, \tag{3.31}$$

which after simplification leads to,

$$\int_0^b \left[rR_n(r)\left(R_m^{''}(r) + \frac{1}{r}R_m^{'}(r)\right) - rR_m(r)\left(R_n^{''}(r) + \frac{1}{r}R_n^{'}(r)\right)\right]dr = 0. \tag{3.32}$$

But on invoking (3.25), we get,

$$(\tau_n^2 - \tau_m^2)\int_0^b rR_m(r)R_n(r)dr = 0. \tag{3.33}$$

Now if $(\tau_n^2 - \tau_m^2) = 0$, which implies $n = m$, then,

$$\int_0^b R_m(r)R_n(r)rdr = \int_0^b rR_m^2(r)dr = \delta_{mn}\Xi_m. \tag{3.34}$$

However if $\tau_n^2 - \tau_m^2 \neq 0$, then

$$\int_0^b r R_m(r) R_n(r) dr = 0. \tag{3.35}$$

Now on combining (3.34) and (3.35), we yield

$$\int_0^b r R_m(r) R_n(r) dr = \delta_{mn} \Xi_n, \tag{3.36}$$

which is orthogonality relation, where δ_{mn} is kronecker delta and,

$$\Xi_n = \frac{b^2}{2} J_0^2(\tau_n b) + \frac{b^2}{2} J_1^2(\tau_n b). \tag{3.37}$$

Consider the duct is radiated with piston moving with velocity U_0, the acoustic radiation will propagate in negative z-direction. The velocity potential for these radiations can be written as,

$$\psi(r, z) = \sum_{n=0}^{\infty} A_n R_n(r) e^{-i\eta_n z}, \tag{3.38}$$

where, $\eta_n = \sqrt{1 - \tau_n^2}$ is the n^{th} wave number. The non-dimensional symmetrical axial velocity distribution of piston can be define by

$$u(r) = \begin{cases} U_0, & 0 \leq r \leq a \\ 0, & a \leq r \leq b \end{cases}, \tag{3.39}$$

where U_0 represents the velocity constant with which piston is moving. Note that the reflected modes amplitudes $A_n : n = 0, 1, 2, 3, ...$ are unknowns. In order to find these we match the propagating modes with radiated modes at $z = 0$. We substitute (3.38) into (3.13) which yields

$$-i \sum_{n=0}^{\infty} A_n \eta_n R_n(r) = u(r), \quad 0 \leq r \leq b. \tag{3.40}$$

On multiplying the above equation by $rR_m(r)$ and on integrating with respect to r, over $0 \leq r \leq b$, to get,

$$-i\sum_{n=0}^{\infty} A_n\eta_n \int_0^b R_n(r)R_m(r)rdr = \int_0^b u(r)R_m(r)rdr. \tag{3.41}$$

Now with the aid of orthogonality relation (3.37) and velocity (3.39), (3.41) can be written as,

$$-i\sum_{n=0}^{\infty} A_n\eta_n\Xi_n\delta_{mn} = U_0\int_0^a R_m(r)rdr, \tag{3.42}$$

which after simplification leads to,

$$A_m = \frac{iU_0D_m}{\eta_m\Xi_m}, \tag{3.43}$$

where,

$$D_m = \int_0^a R_m(r)rdr. \tag{3.44}$$

3.2 Numerical Illustration

Here the problem is discussed numerically. For absorbing lining the following values of specific impedance are considered as,

$$\beta^{-1} = i\xi - \eta,$$

are reasonably representative. For numerical computation, speed of sound in air and density of compressible fluid remain fixed

$$c = 343m/sec, \quad \rho = 1.2043kg/m^3,$$

whereas the dimensional radius of circular regions and properties of porous material are varied. To plot Figs 3.2-3.5, the dimensional radius are taken as $\overline{a} = 0.2m$ *and* $\overline{b} = 0.3m$. In Figs 3.2-3.3 the fibrous material is aligned along the

circular region of the duct while for Figs 3.4-3.5 the perforated material is sticked along the circular walls.

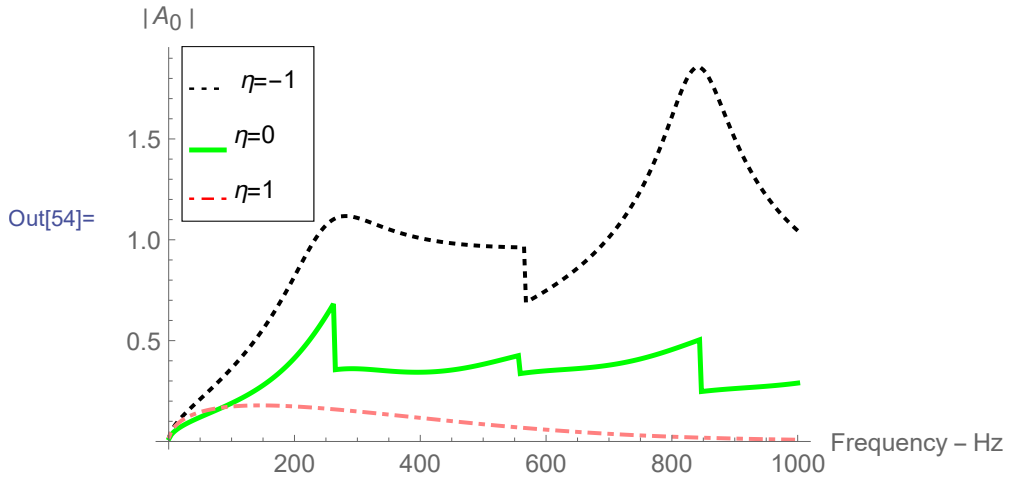

(a)

FIGURE 3.2: Absolute value of fundamental mode amplitude verses frequency for $N = 20, \overline{a} = 0.2m$ and $\overline{b} = 0.3m$ with fibrous sheet $\xi = 0.5$.

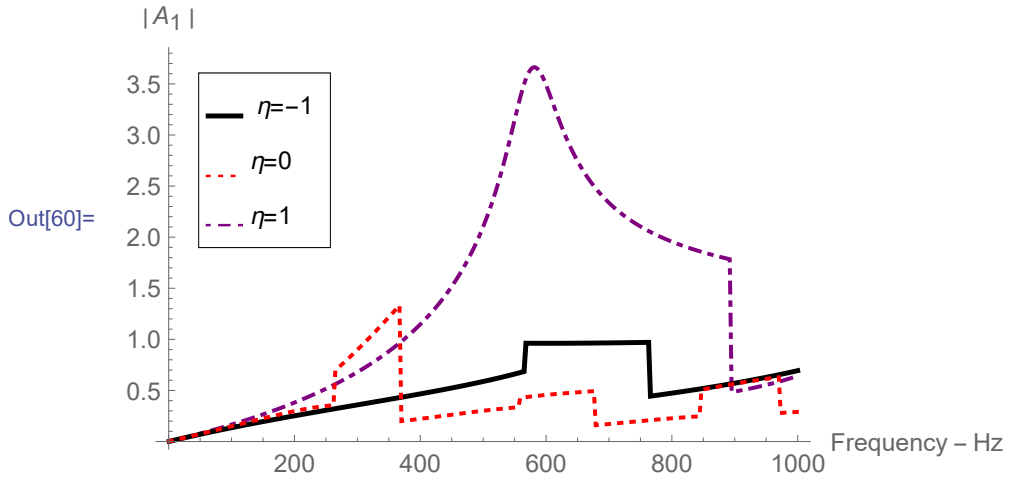

(a)

FIGURE 3.3: Absolute value of secondary mode amplitude verses frequency for $N = 20, \overline{a} = 0.2m$ and $\overline{b} = 0.3m$ with fibrous sheet $\xi = 0.5$.

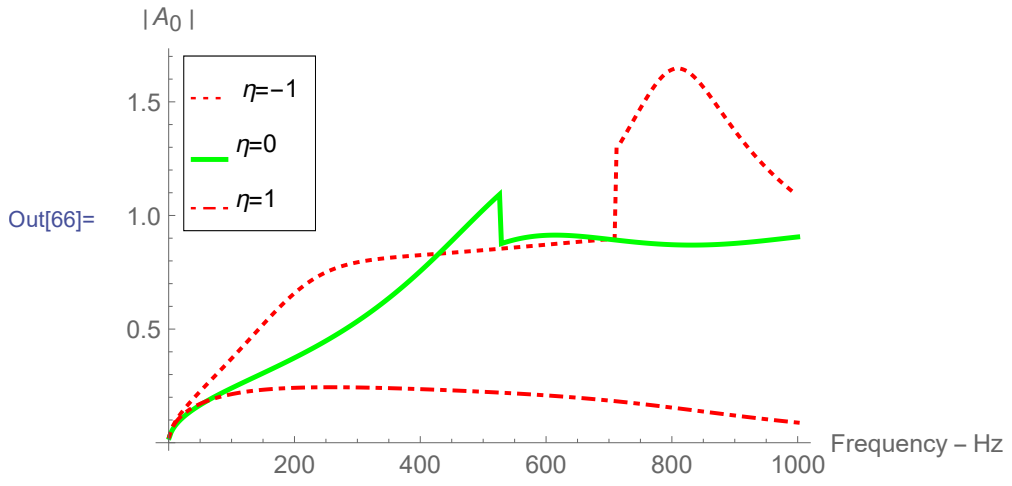

(a)

FIGURE 3.4: Absolute value of fundamental mode amplitude verses frequency for $N = 20, \overline{a} = 0.2m$ and $\overline{b} = 0.3m$ with perforated sheet $\xi = 1$.

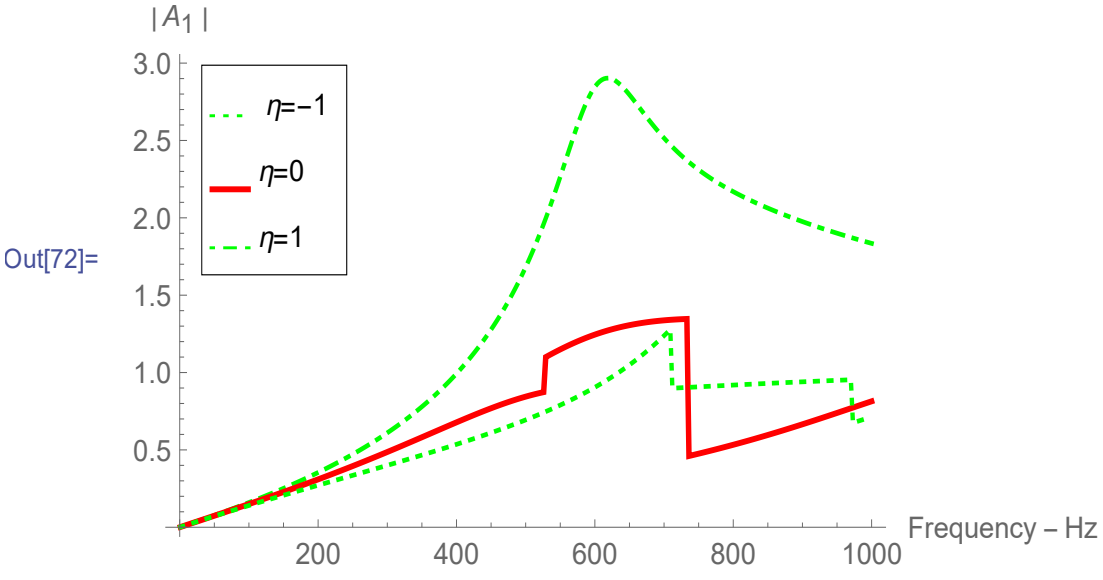

(a)

FIGURE 3.5: Absolute value of secondary mode amplitude verses frequency for $N = 20, \overline{a} = 0.2m$ and $\overline{b} = 0.3m$ with perforated sheet $\xi = 1$.

From the graphs in Figs 3.2 to 3.5, it can be seen that, by changing the properties of bounding walls, the propagating amplitudes are changed. The following values for the specific impedance $(i\xi - \eta)$ are assumed for fibrous sheet:

- $\xi = 0.5 \quad -1.0 \leq \eta \leq 3.0$

and for perforated sheet:

- $\xi = 1, quad - 1.0 \leq \eta \leq 3.0.$

Now by changing the radii of circular regions to $\overline{a} = 0.3m$ and $\overline{b} = 0.4m$, the scattering amplitudes against frequency are shown in Figs 3.6-3.9. Results for both fibrous and perforated materials are displayed. From these graphs it is found that, by changing the values of dimensional radii of circular regions and the properties of bounding walls the resulting amplitudes are changed.

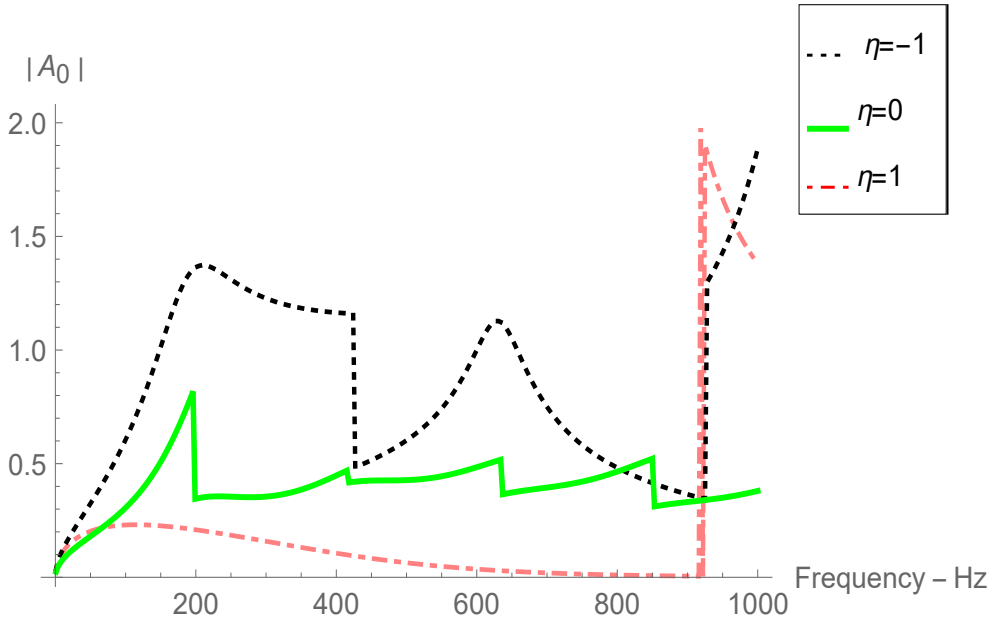

(a)

FIGURE 3.6: Absolute value of fundamental mode amplitude verses frequency for $N = 20, \overline{a} = 0.3m$ and $\overline{b} = 0.4m$ with fibrous sheet $\xi = 0.5$.

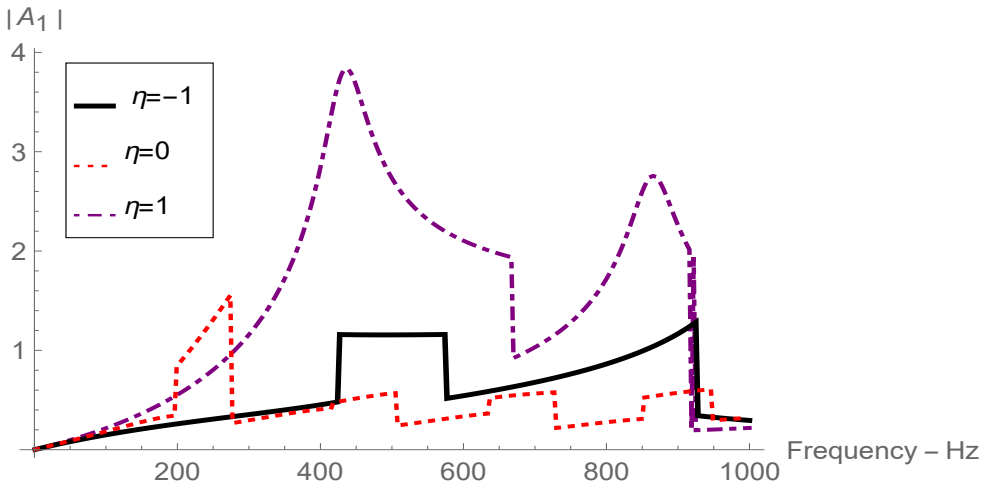

(a)

FIGURE 3.7: Absolute value of secondary mode amplitude verses frequency for $N = 20, \overline{a} = 0.3m$ and $\overline{b} = 0.4m$ with fibrous sheet $\xi = 0.5$.

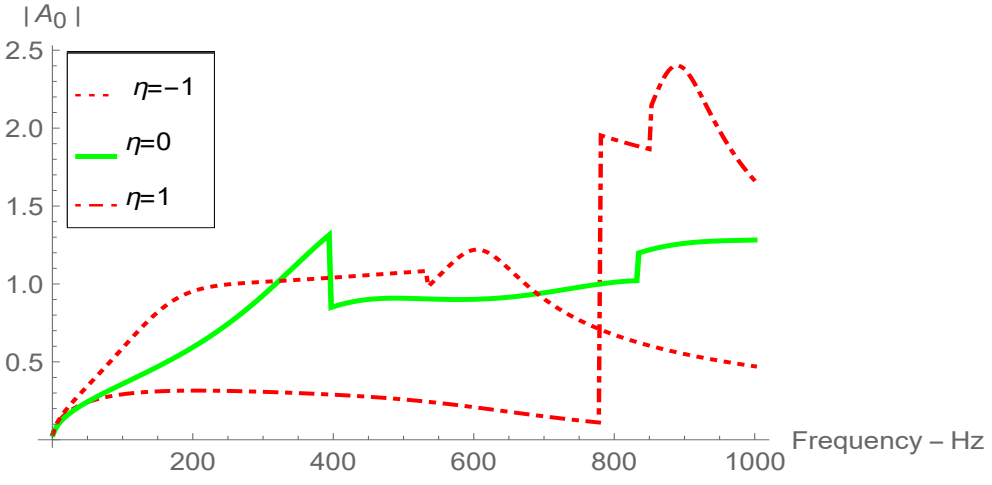

(a)

FIGURE 3.8: Absolute value of fundamental mode amplitude verses frequency for $N = 20, \overline{a} = 0.3m$ and $\overline{b} = 0.4m$ with perforated sheet $\xi = 1$.

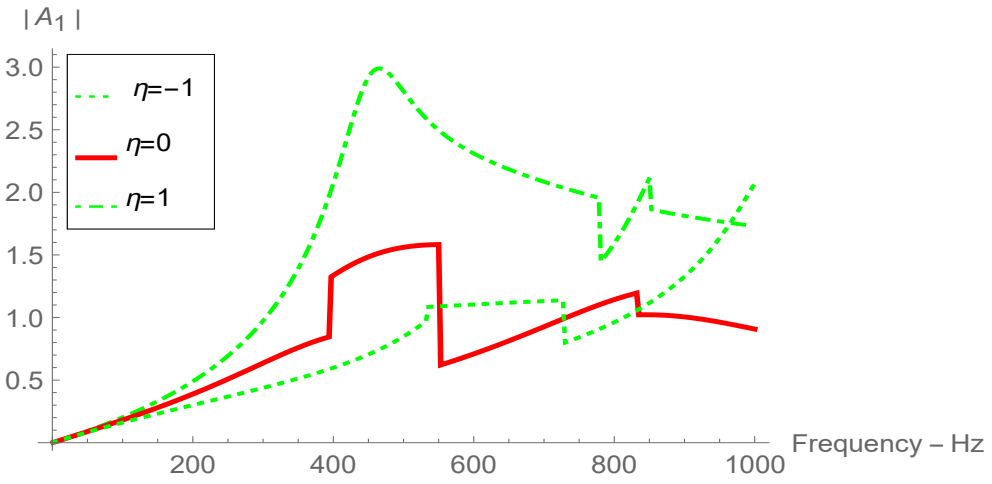

(a)

FIGURE 3.9: Absolute value of secondary mode amplitudes Amplitudes verses frequency for $N = 20, \overline{a} = 0.3m$ and $\overline{b} = 0.4m$ with perforated sheet $\xi = 1$.

3.3 Acoustic Scattering in a Discontinues Waveguide Radiated with Duct Mode Forcing

Here the acoustic scattering in discontinuous cylindrical waveguide involving porous lining is assumed. The waveguide is stretched infinitely along z-direction and comprises two duct sections of different radii a and b where $b > a$. The physical configuration is as shown in Figure (3.10).

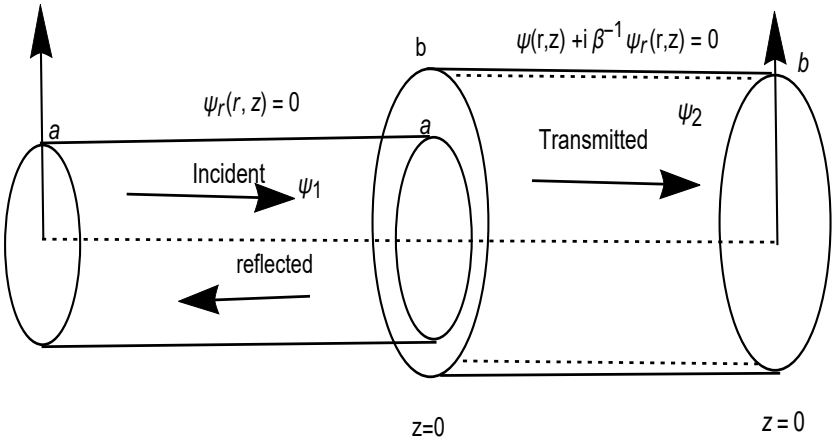

FIGURE 3.10: The geometrical configuration of waveguide.

The circular wall of the left hand duct along z-direction contains rigid type wall condition along the circular region of radius $\overline{r} = \overline{a}$, whilst the right hand duct comprises absorbing lining at radius $\overline{r} = \overline{b}$. The inside of the ducts are filled with compressible fluid of density ρ and sound speed c, whereas, the outer side of ducts contained in *vacuo*.

The harmonic time dependence $e^{-i\omega\overline{t}}$ is considered and is supressed throughout.

Moreover the governing BVP is non-dimensionalized in similar fashion as detailed in the previous section. So here we only discuss the non-dimensional form of the BVP.

Consider an incident wave of duct mode is propagating from negative z-direction towards $z = 0$ in cylindrical waveguide. At $z = 0$ it will scatter into infinite number of reflected and transmitted waves. The field potential in the waveguide region is given by,

$$\psi(r,z) = \begin{cases} \psi_1(r,z), & 0 \le r \le a, z \le 0 \\ \psi_2(r,z), & 0 \le r \le b, z \ge 0 \end{cases}, \tag{3.45}$$

where $\psi_1(r,z)$ and $\psi_2(r,z)$ represent the field potentials in left hand and right hand duct respectively. These field potentials satisfy the non-dimensional Helmholtz's equation,

$$\left\{ \frac{\partial^2}{\partial r^2} + \frac{1}{r}\frac{\partial}{\partial r} + \frac{\partial^2}{\partial z^2} + 1 \right\} \psi(r,z) = 0, \quad \overline{z} < \overline{0}, \quad \overline{0} \le r \le \overline{a}. \tag{3.46}$$

For left hand duct region the rigid type of boundary condition is

$$\frac{\partial \psi_1}{\partial r}(r,z) = 0, \quad r = a, \quad z < 0. \tag{3.47}$$

In the right hand duct region the impedance type boundary condition is

$$\psi_2(r,z) + i\beta^{-1}\frac{\partial \psi_2}{\partial r}(r,z) = 0, \quad r = b, \quad z > 0. \tag{3.48}$$

The step discontinuity along $a \le r \le b$ at $z = 0$ is acoustically rigid, that is

$$\frac{\partial \psi_2}{\partial z} = 0, \quad z = 0, \quad a \le r \le b. \tag{3.49}$$

By using the separation of variable technique, (3.46) to (3.49) yield the eigenfunction expansion of field potentials as

$$\psi_1 = F_0 R_{10} e^{iz} + \sum_{n=0}^{\infty} A_n R_{1n}(r) e^{-i\eta_n z} \tag{3.50}$$

and

$$\psi_2 = \sum_{n=0}^{\infty} B_n R_{2n}(r) e^{is_n z}, \tag{3.51}$$

where $\eta_n = \sqrt{1-\tau_n^2}$ and $s_n = \sqrt{1-\gamma_n^2}$ are the wave numbers of left and right hand ducts respectively. The corresponding eigenfunction $R_{1n}(r) = J_0(\tau_n r)$ and $R_{2n}(r) = J_0(\gamma_n r)$ are orthogonal and satisfy the orthogonality relation. The eigenvalue τ_n and γ_n are the roots of the dispersion relation,

$$J_0(\tau_n a) = 0 \tag{3.52}$$

and

$$J_0(\gamma_n b) - i\beta^{-1}\gamma_n J_1(\gamma_n b) = 0. \tag{3.53}$$

The orthogonality relations for left and right hand ducts are given below

$$\int_0^a r R_{1m}(r) R_{1n}(r) dr = \delta_{mn}\Xi_{1n}, \tag{3.54}$$

and

$$\int_0^b r R_{2m}(r) R_{2n}(r) dr = \delta_{mn}\Xi_{2n}, \tag{3.55}$$

where,

$$\Xi_{1n} = \frac{a^2}{2} J_0^2(\tau_n a), \tag{3.56}$$

and

$$\Xi_{2n} = \frac{b^2}{2}\left\{J_0^2(\gamma_n b) + J_1^2(\gamma_n b)\right\}. \tag{3.57}$$

Note that first term on the right hand side of (3.50) represents the fundamental incident mode with a forcing F_n, whereas the second term shows the reflected field. However (3.51) stand for the transmitted field in right hand duct. Note that the coefficient $\{A_n, B_n\}$, $n = 0, 1, 2, ...$ are still unknowns. These are found through the MM procedure which is discussed in next section.

3.3.1 Mode-Matching Solution

The scattering amplitudes can be determined by using the matching conditions of pressures and normal velocities at interfaces. These conditions define the continuities of pressure and velocities across the regions at interface, there are

$$\psi_1(r,0) = \psi_2(r,0), \quad for \quad 0 \le r \le a, \tag{3.58}$$

$$\frac{\partial \psi_2}{\partial z}(r,0) = \begin{cases} \frac{\partial \psi_1}{\partial z}(r,0), & 0 \le r \le a \\ 0, & a \le r \le b \end{cases}. \tag{3.59}$$

By substituting (3.50) and (3.51) into (3.58), we get

$$F_0 R_{10}(r) + \sum_{n=0}^{\infty} A_n R_{1n}(r) = \begin{cases} \sum_{n=0}^{\infty} B_n R_{2n}(r), & 0 \le r \le a \\ 0 & a \le r \le b \end{cases}. \tag{3.60}$$

We multiply (3.60) with $rR_{1m}(r)$ and then integrate over $0 \le r \le a$, we found

$$\begin{aligned} F_0 \int_0^a R_{10}(r) R_{1m}(r) r dr + \sum_{n=0}^{\infty} A_n \int_0^a R_{1n}(r) R_{1m}(r) r dr \\ = \sum_{n=0}^{\infty} B_n \int_0^a R_{1m}(r) R_{2n}(r) r dr. \end{aligned} \tag{3.61}$$

The left hand integral of (3.61) is evaluated by using the orthogonality relation (3.56). Therefore, after simplification, (3.61) takes the form

$$A_m = -F_0 \delta_{m0} + \frac{1}{\Xi_{1m}} \sum_{n=0}^{\infty} B_n Q_{mn}, \tag{3.62}$$

where,

$$Q_{mn} = \int_0^a R_{1m}(r) R_{2n}(r) r dr. \tag{3.63}$$

For $m \neq n$,

$$Q_{mn} = \frac{\gamma_n J_1(\gamma_n r) J_0(\tau_m r) - \tau_m J_0(\tau_m r) J_0(\gamma_n r)}{\gamma_n^2 - \tau_m^2}. \tag{3.64}$$

If $m = n$, then (3.63) gives,

$$Q_{mn} = \frac{a^2 J_0(\tau_m a)}{2}. \tag{3.65}$$

Now, we substitute (3.50) and (3.51) into normal velocity condition to get,

$$\sum_{n=0}^{\infty} iB_n s_n R_{2n}(r) = \begin{cases} iF_0 R_{10}(r) - i\sum_{n=0}^{\infty} A_n \eta_n R_{1n}(r) & 0 \le r \le a \\ 0 & a \le r \le b. \end{cases} \tag{3.66}$$

By multiplying (3.66) with $rR_{2m}(r)$, integrating over $0 \le r \le b$, we found

$$\begin{aligned} B_n s_n \int_0^b R_{2n}(r) R_{2m}(r) r dr = F_0 \int_0^a R_{10}(r) R_{2m}(r) r dr \\ -i\sum_{n=0}^{\infty} A_n \eta_n \int_0^a R_{1n}(r) R_{2m}(r) r dr. \end{aligned} \tag{3.67}$$

To evaluate (3.67), we invoke orthogonality relation (3.57) to get

$$B_m = \frac{F_0 Q_{0m}}{s_m \Xi_{2m}} - \frac{1}{s_m \Xi_{2m}} \sum_{n=0}^{\infty} A_n \eta_n Q_{mn}. \tag{3.68}$$

In this way (3.62) and (3.68) lead to a system of linear algebraic equations which are truncated and solved simultaneously.

3.3.2 Energy Expression

The expressions are required to define energies in the waveguide. The dimensional energy $\overline{\mathcal{E}}$ is defined by scattering [36]

$$\overline{\mathcal{E}} = 2\pi\omega\rho Re\left[\int_\Omega i\overline{\psi}\left(\frac{\partial\overline{\psi}}{\partial\overline{z}}\right)^* \overline{r}d\overline{r}\right], \tag{3.69}$$

where Ω is the region. By non-dimensionalizing under the transformation given in (3.5) we get

$$\overline{\mathcal{E}} = \frac{2\pi\omega^3\rho}{k^5} Re\left[\int_\Omega i\psi\left(\frac{\partial\psi}{\partial z}\right)^* r dr\right], \tag{3.70}$$

where ω is the radian frequency and $\omega = ck$, k is the fluid wave number and c is the sound speed. By using this value of ω in equation (3.70), we have

$$\overline{\mathcal{E}} = \frac{2\pi c^3 \rho}{k^2} Re\left[\int_\Omega i\psi \left(\frac{\partial \psi}{\partial z}\right)^* r dr\right]. \tag{3.71}$$

Now, we can write the (3.71) as

$$\overline{\mathcal{E}} = \frac{2\pi c^3 \rho}{k^2} \mathcal{E}, \tag{3.72}$$

where,

$$\mathcal{E} = Re\left[\int_\Omega i\psi \left(\frac{\partial \psi}{\partial z}\right)^* r dr\right]. \tag{3.73}$$

Note that, (3.73) shows the energy carried by an individual propagating mode with non-dimensional setting. Now for incident field as $\psi_{inc} = F_0 R_{10} e^{iz}$.
Equation (3.73) leads to incident power

$$\mathcal{E}_{inc} = Re\left\{F_0 \int_0^a i R_{10}(r) e^{iz_0} \left(-iF_0 R_{10}(r) e^{-iz_0}\right)^* r dr\right\}, \tag{3.74}$$

$$\mathcal{E}_{inc} = Re\left\{F_0^2 \int_0^a R_{10}(r) R_{10}(r) r dr\right\}. \tag{3.75}$$

By using orthogonality relation (3.56)in above expression we get

$$\mathcal{E}_{inc} = Re\left\{\Xi_0 \mid F_0 \mid^2 \frac{a^2}{2}\right\}. \tag{3.76}$$

We choose $\mid F_0 \mid^2 = 1/\Xi_0$ to scale the incident power at unity which yields

$$F_0 = \frac{\sqrt{2}}{a}. \tag{3.77}$$

Likewise to calculate the reflected power in inlet we use the reflected field

$$\psi_{ref} = \sum_{n=0}^{\infty} A_n R_{1n}(r) e^{-i\eta_n z}, \tag{3.78}$$

into (3.73), which gives

Reflected energy flux =

$$Re\left[i\int_0^a\left(\sum_{n=0}^{\infty}A_nR_{1n}e^{-i\eta_n}\right)\times\left(\sum_{m=0}^{\infty}-A_mR_{1m}i\eta_me^{-i\eta_mz}\right)^*\right]rdr. \tag{3.79}$$

Reflected energy flux =

$$-\,Re\left[\int_0^a\sum_{m=0}^{\infty}\sum_{n=0}^{\infty}A_nA_m^*R_{1m}^*R_{1n}\eta_m^*e^{-i(\eta_n-\eta_m^*)z}rdr\right].. \tag{3.80}$$

Note that, as $\tau_n; n = 0, 1, 2....$ are real which implies $R_{1m} = J_0(\tau_m r)$ to real, thus $R_{1m}^* = R_{1m}$.

Reflected energy flux =

$$-\,Re\left[\sum_{m=0}^{\infty}\sum_{n=0}^{\infty}A_nA_m^*\eta_m^*e^{-i(\eta_n-\eta_m^*)z}\int_0^a R_{1n}R_{1m}rdr\right]. \tag{3.81}$$

On using orthogonality relation (3.56).

$$Reflected\ energy\ flux = -Re\left[\sum_{m=0}^{\infty}\sum_{n=0}^{\infty}A_nA_m^*\eta_m^*e^{-i(\eta_n-\eta_m^*)z}\delta_{mn}\Xi_{1m}\right], \tag{3.82}$$

or

$$Reflected\ energy\ flux = -Re\left[\sum_{n=0}^{\infty}\mid A_n\mid^2\eta_n^*e^{-i(\eta_n-\eta_n^*)z}\Xi_{1m}\right]. \tag{3.83}$$

As $\eta_n = \sqrt{1-\tau_n}$ is either real or pure imaginary. For real η_n the above equation (3.83) gives

$$Reflected\ energy\ flux = -Re\left[\sum_{n=0}^{\infty}\mid A_n\mid^2\eta_n\Xi_{1n}\right]. \tag{3.84}$$

For pure imaginary, (3.83) yields $\mathcal{E}_r = 0$. Thus the reflected energy flux

$$Reflected\ energy\ flux = -\mathcal{E}_r, \tag{3.85}$$

where

$$\mathcal{E}_r = Re\left[\sum_{n=0}^{\infty} \mid A_n \mid^2 \eta_n \Xi_{1n}\right]. \tag{3.86}$$

The negative sign in (3.85) represents the energy flux in negative z-direction. It is important to note that transmitted power in right hand duct cannot be found since it involve porous lining along that region which yields γ_n to be complex values and thus the resulting $R_{2n}(\gamma_n r)$ will also be complex. Moreover some power will be absorbed depending upon the properties of lining. Thus conserve power identity leads to

$$\textit{power in left hand region} = \textit{power in right hand region} \tag{3.87}$$

$$1 = \mathcal{E}_r + \mathcal{E}_{abs}, \tag{3.88}$$

which implies

$$\mathcal{E}_{abs} = 1 - \mathcal{E}_r. \tag{3.89}$$

3.3.3 Numerical Illustration

Here the system of equations (3.62) and (3.68) are truncated upto N terms and are solved numerically. The computations are performed in Mathematica. For computation, the physical dimensional heights are fixed as: $\overline{a} = 0.2m$, and $\overline{b} = 0.28m$, for the case without cavity inclusion. The compressible fluid density $\rho = 1.2043kgm^{-3}$ and sound speed $c = 343ms^{-1}$ remain unchanged. The specific admittance $\beta^{-1} = i\zeta - \eta$, where $\zeta = 0.5$, $-1 \leq \eta \leq 3$ for fibrous sheet and $0 < \zeta < 3$, $-1 \leq \eta \leq 3$ for perforated sheet is considered. In Figs. 3.11-3.14, the normal velocities and pressures are plotted at $z = 0$. From the graphs presented in Figs. 3.11-3.14, it can be seen that the real and imaginary parts of normal velocities and pressures match exactly as considered in matching conditions (3.58) and (3.59). It clearly justifies the accuracy of truncated solution and presented algebra.

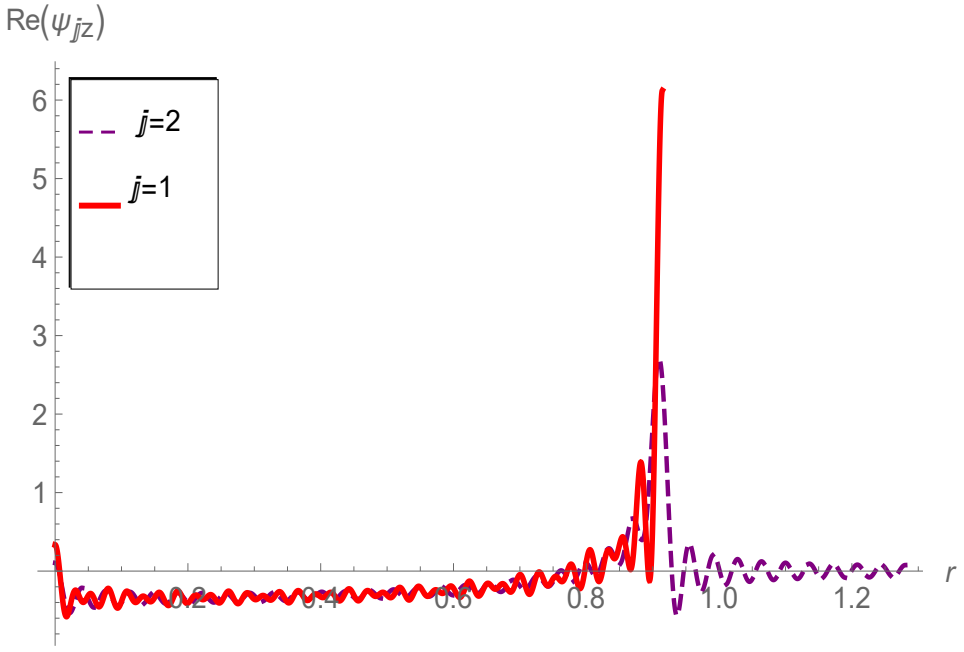

(a)

FIGURE 3.11: At $z = 0$, the real parts for normal velocities against radius r where $\overline{a} = 0.2m, \overline{b} = 0.28m$, $f = 250Hz$ and $N = 70$.

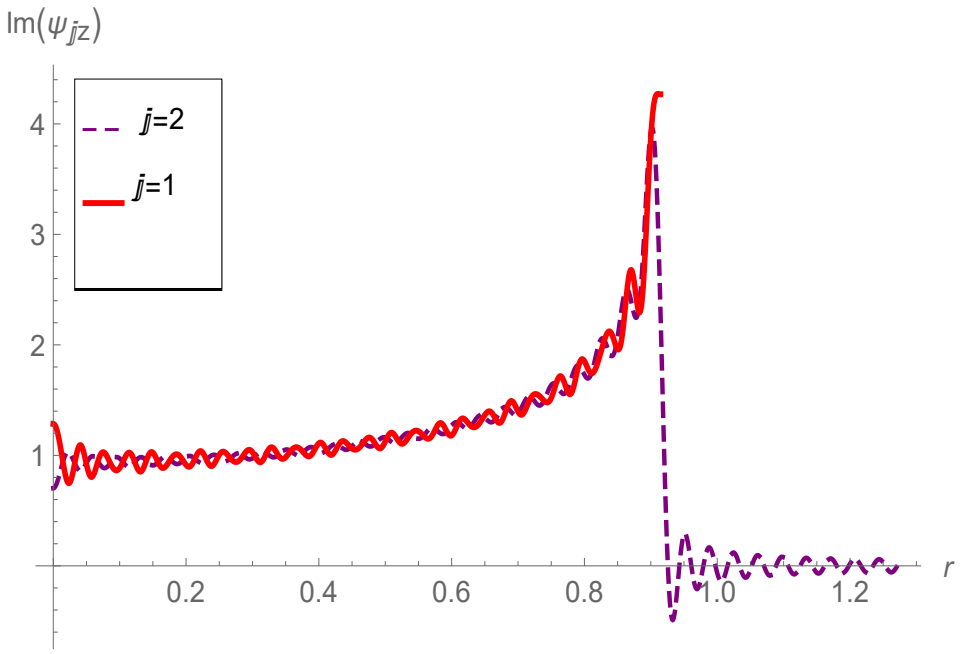

(a)

FIGURE 3.12: At $z = 0$, the imaginary parts for normal velocities against radius r where $\overline{a} = 0.2m, \overline{b} = 0.28m$, $f = 250Hz$ and $N = 70$.

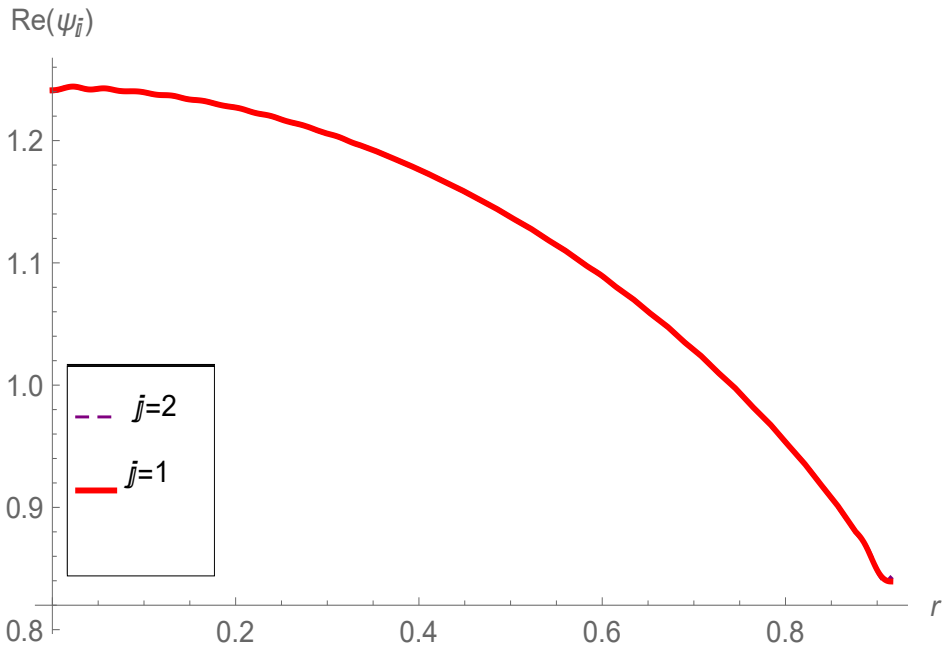

(a)

FIGURE 3.13: At $z = 0$, the real parts for pressures against radius r where $\overline{a} = 0.2m, \overline{b} = 0.28m$, $f = 250Hz$ and $N = 70$.

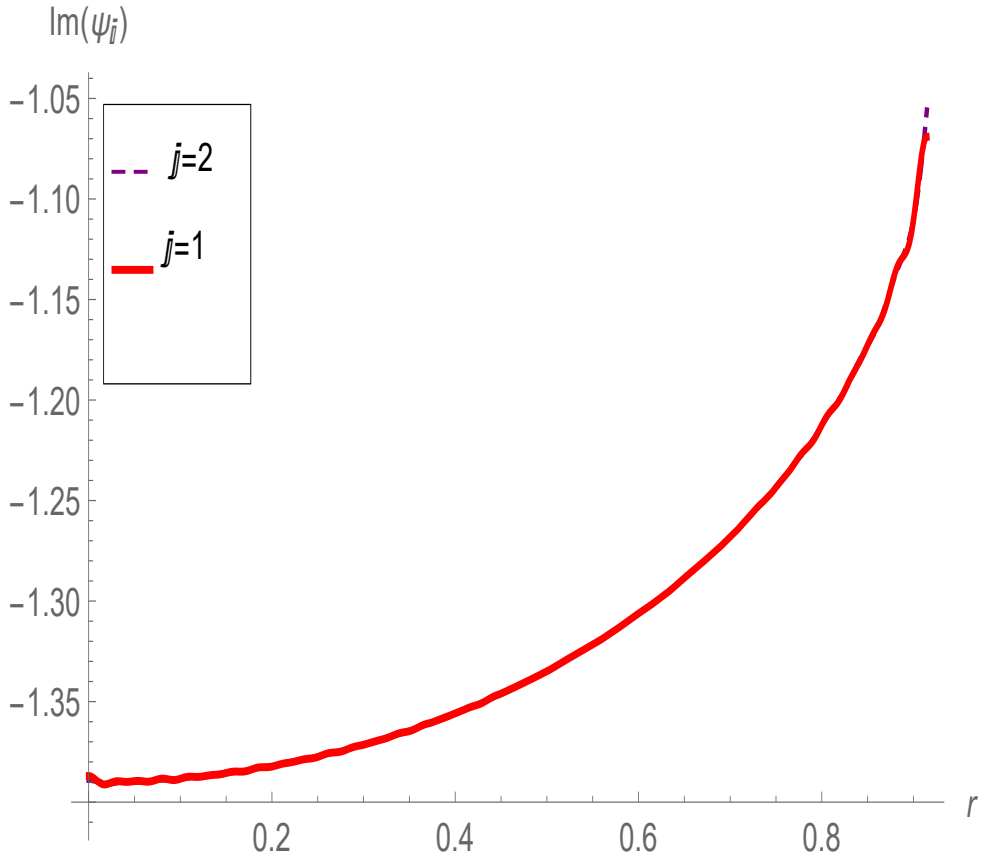

(a)

FIGURE 3.14: At $z = 0$, the imaginary parts for pressures against radius r where $\overline{a} = 0.2m, \overline{b} = 0.28m$, $f = 250Hz$ and $N = 70$.

To see the physical behavior of reflected energy against frequency the Figs 3.15-318 are displayed. In Figs 3.15-3.18, the reflected energy verses by fixing the radii of circular regions at $\overline{a} = 0.2m \quad and \quad \overline{b} = 0.28m$ and varying the properties of absorbing material is shown. The results with fibrous material for which $\zeta = 0.5$ and $-1 \leq \eta \leq 3$ are shown in Figs 3.15 whilst the results with perforated material are presented in Figs 3.16.

Likewise in Figs 3.17-3.18, the reflected energy is plotted against frequency by changing the radii of circular regions to $\overline{a} = 0.1m \quad and \quad \overline{b} = 0.2m$. The results for both fibrous and perforated materials are displayed. It can be seen that by decreasing the radii of circular regions reflection is increased.

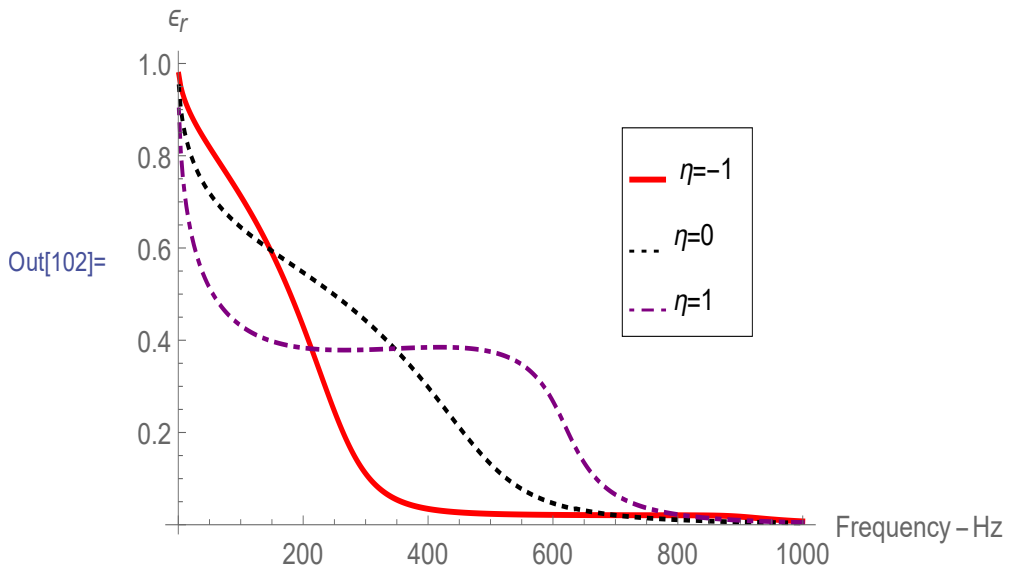

(a)

FIGURE 3.15: The reflected power against frequency for fibrous sheet $\zeta = 0.5$, where, $\overline{a} = 0.2m$, $\overline{b} = 0.28m$ and $N = 20$

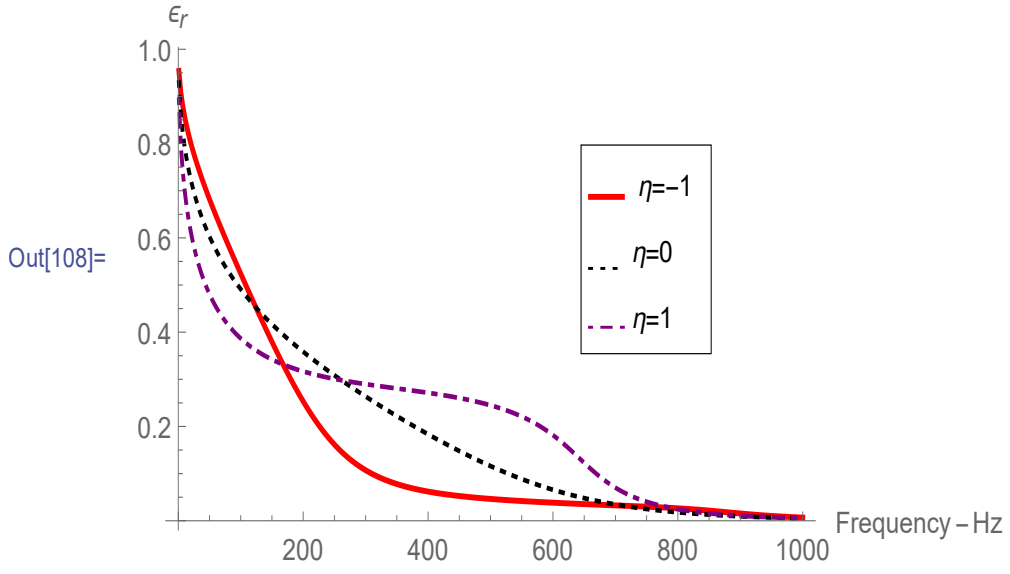

(a)

FIGURE 3.16: The reflected power against frequency for perforated sheet $\zeta = 1$ where, $\overline{a} = 0.2m$, $\overline{b} = 0.28m$ and $N = 20$

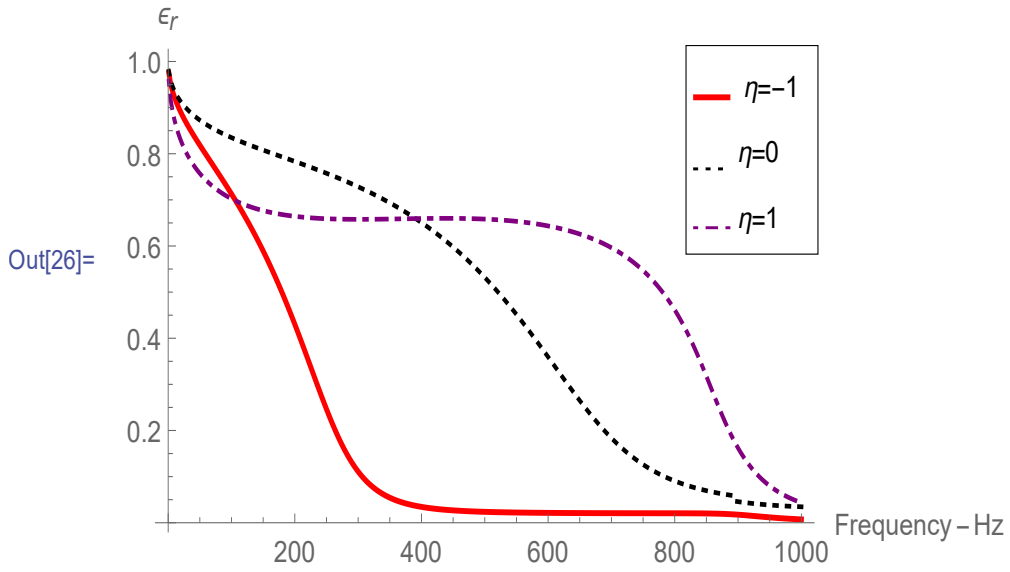

(a)

FIGURE 3.17: The reflected power against frequency for fibrous sheet $\zeta = 0.5$, where, $\overline{a} = 0.1m$, $\overline{b} = 0.2m$ and $N = 20$

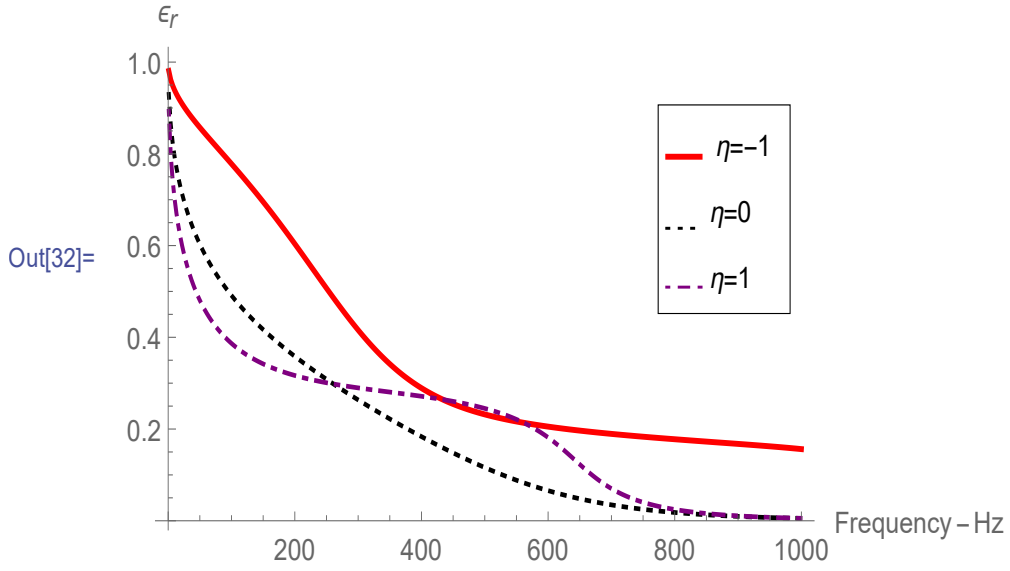

(a)

FIGURE 3.18: The reflected power against frequency for perforated sheet $\zeta = 1$ where, $\overline{a} = 0.1m$, $\overline{b} = 0.2m$ and $N = 20$

Chapter 4

Scattering through Lined Cylindrical Expansion Chamber

The waveguide discussed in this chapter comprises three duct regions inlet, outlet and expansion chamber. The inlet and outlet regions are joined with expansion chamber by means of flanges, at interfaces.
The inside of the chamber contains absorbent lining. The governing BVP is solved by using MM technique. In next sections BVP and MM solution are presented.

4.1 Boundary Value Problem

Acoustic scattering in a discontinuous cylindrical waveguide containing step discontinuity and absorbing lining is assumed. The waveguide is stretched infinitely along z-direction and comprises three duct sections of different radii a , b and h where $b > a$ and $a > h$ the physical configuration is as shown in figure below.

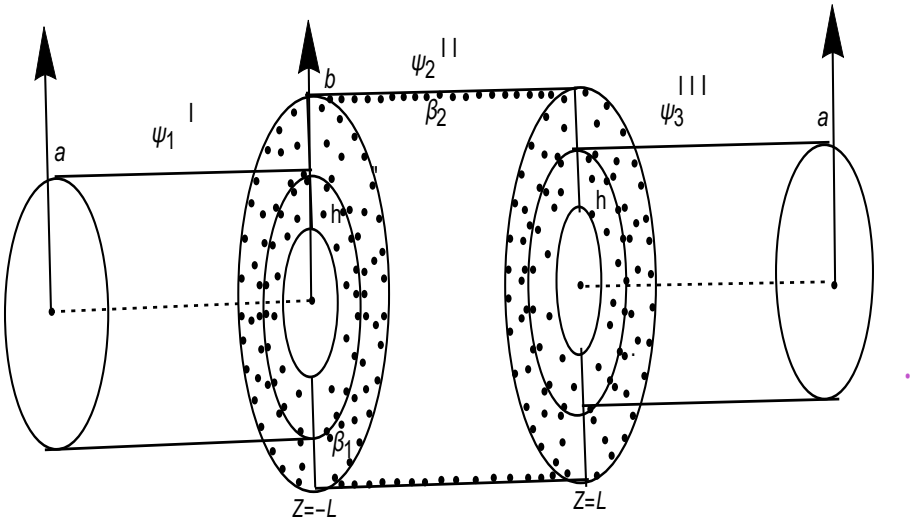

FIGURE 4.1: The geometrical configuration of duct.

The inside cylindrical walls of the inlet and outlet ducts along z-direction contains rigid type wall condition at radius $\overline{r} = \overline{a}$. Whilst, the finite expansion chamber comprises the impedance type wall condition. Inside of the ducts are filled with compressible fluid of density ρ and sound speed c, whereas, the outer side of ducts is in *vacuo*.

Here the harmonic time dependence $e^{-i\omega\overline{t}}$ is considered and we only discuss the non-dimensional form of the BVP. Consider an incident wave of duct mode is propagating from negative z-direction towards $|z| = L$ in cylindrical waveguide, where it scatter into infinite number of reflected and transmitted waves. The field potential in the waveguide region can be given as

$$\psi(r,z) = \begin{cases} \psi_1(r,z), & 0 \le r \le a, z \le -L \\ \psi_2(r,z), & 0 \le r \le b, z \ge -L \\ \psi_3(r,z), & 0 \le r \le a, z \le L \end{cases}, \tag{4.1}$$

where $\psi_1(r,z)$, $\psi_2(r,z)$ and $\psi_3(r,z)$ represent the field potentials in the inlet, expansion chamber and outlet duct, respectively. These field potentials satisfy the non-dimensional Helmholtz's equation

$$\left\{\frac{\partial^2}{\partial r^2}+\frac{1}{r}\frac{\partial}{\partial r}+\frac{\partial^2}{\partial z^2}+1\right\}\psi(r,z)=0. \tag{4.2}$$

For inlet duct region the non-dimensional rigid type of boundary condition is,

$$\frac{\partial \psi_1}{\partial r}(r,z)=0, \quad r=a, \quad z\leq -L. \tag{4.3}$$

In the expansion chamber region the non-dimensional impedance type boundary condition is

$$\psi_2(r,z)+i\beta^{-1}\frac{\partial \psi_2}{\partial r}(r,z)=0, \quad r=b, \quad z\leq L. \tag{4.4}$$

The surfaces of flanges towards inlet/outlet ducts are assumed to be acoustically rigid

$$\frac{\partial \psi_1}{\partial z}(-L,r)=0, \quad h\leq r\leq a, \tag{4.5}$$

$$\frac{\partial \psi_3}{\partial z}(L,r)=0, \quad h\leq r\leq b. \tag{4.6}$$

wherease, the surfaces of flanges step inside of the expansion chamber are lined with absorbing lining.

$$\psi_2(r,z)-i\beta^{-1}\frac{\partial \psi_2}{\partial r}(r,z)=0, \quad z=-L, \quad h\leq r\leq b, \tag{4.7}$$

$$\psi_2(r,z)+i\beta^{-1}\frac{\partial \psi_2}{\partial r}(r,z)=0, \quad z=L, \quad h\leq r\leq b. \tag{4.8}$$

In next section, the MM solution is given.

4.1.1 Mode-Matching Solution

By using the separation of variable method, the eigenfunction expansions of field potentials in duct regions are found as:

$$\psi_1 = F_0 R_{10} e^{i(z+L)} + \sum_{n=0}^{\infty} A_n R_{1n}(r) e^{-i\eta_n(z+L)}, \tag{4.9}$$

$$\psi_2 = \sum_{n=0}^{\infty} \left(B_n e^{is_n z} + C_n e^{-is_n z} \right) R_{2n}(r), \tag{4.10}$$

and

$$\psi_3 = \sum_{n=0}^{\infty} D_n R_{1n}(r) e^{i\eta_n(z-L)}, \tag{4.11}$$

where, $\psi_1(r,z)$ represents the reflected field potential in inlet, $\psi_3(r,z)$, shows the transmitted filed potential in outlet and $\psi_2(r,z)$ represents the field potential in expansion chamber. The eigenfunctions of these regions satisfy the following orthogonality relations:

$$\int_0^a r R_{1m}(r) R_{1n}(r) dr = \delta_{mn} \Xi_{1n} \tag{4.12}$$

and

$$\int_0^b r R_{2m}(r) R_{2n}(r) dr = \delta_{mn} \Xi_{2n}, \tag{4.13}$$

where,

$$\Xi_{1n} = \frac{a^2}{2} J_0^2(\tau_n a) \tag{4.14}$$

and

$$\Xi_{2n} = \frac{b^2}{2} \left\{ J_0^2(\gamma_n b) + J_1^2(\gamma_n b) \right\}. \tag{4.15}$$

The coefficients $\{A_n, B_n, C_n, D_n\}$, $n = 0, 1, 2, 3, ...$ are still unknowns. These are found by using MM procedure. The normal velocities across the regions interfaces can be given as,

$$\frac{\partial \psi_1}{\partial z}(r, -L) = \begin{cases} \frac{\partial \psi_2}{\partial z}(r, -L), & 0 \le r \le h \\ 0, & h \le r \le a. \end{cases} \tag{4.16}$$

$$\frac{\partial \psi_3}{\partial z}(r,L) = \begin{cases} \frac{\partial \psi_2}{\partial z}(r,L), & 0 \le r \le h \\ 0, & h \le r \le a \end{cases}. \tag{4.17}$$

By substituting (4.9) and (4.10) into (3.19), we get

$$F_0 R_{10} - \sum_{n=0}^{\infty} A_n \eta_n R_{1n}(r) = \begin{cases} \sum_{n=0}^{\infty} \left\{ B_n s_n e^{-is_n L} - C_n s_n e^{is_n L} \right\} R_{2n}(r) & 0 \le r \le a \\ 0, & h \le r \le a \end{cases}. \tag{4.18}$$

On multiplying (4.18) by $rR_{1m}(r)$ and integrating with respect to r over $0 \le r \le a$, the resulting equation is

$$F_0 \int_0^a R_{10}(r) R_{1m}(r) r dr - \sum_{n=0}^{\infty} A_n \eta_n \int_0^a R_{1n}(r) R_{1m}(r) r dr$$

$$= \sum_{n=0}^{\infty} \left\{ B_n s_n e^{-is_n L} - C_n s_n e^{is_n L} \right\} \int_0^h R_{2n}(r) R_{1m}(r) r dr. \tag{4.19}$$

After simplification of the above equation and using orthogonality relation given in (4.14), we get

$$A_m = \frac{F_0 \delta_{0m}}{\eta_m} - \frac{1}{\eta_m \Xi_{1m}} \sum_{n=0}^{\infty} \left\{ B_n e^{-is_n L} - C_n e^{is_n L} \right\} s_n Q_{nm}. \tag{4.20}$$

By substituting (4.10) and (4.11) into (4.17) we obtain

$$\sum_{n=0}^{\infty} D_n \eta_n R_{1n}(r) = \begin{cases} \sum_{n=0}^{\infty} \left\{ B_n e^{is_n L} - C_n e^{-is_n L} \right\} s_n R_{2n}(r) & 0 \le r \le h \\ 0 & h \le r \le a. \end{cases} \tag{4.21}$$

We multiply (4.21 with $rR_{1m}(r)$ and integrate over $0 \le r \le a$, we get

$$D_n \eta_n \int_0^a R_{1n}(r) R_{1m}(r) r dr =$$

$$\sum_{n=0}^{\infty} \left\{ B_n e^{is_n L} - C_n e^{is_n L} \right\} s_n \int_0^h R_{2n}(r) R_{1m}(r) r dr. \tag{4.22}$$

After simplification the above expression we get

$$D_m = \frac{1}{\eta_m \Xi_{1m}} \sum_{n=0}^{\infty} \left\{ B_n e^{is_n L} - C_n e^{-is_n L} \right\} s_n Q_{nm}. \tag{4.23}$$

By adding (4.20) and (4.23) we obtain

$$A_m + D_m = \frac{F_0 \delta_{0m}}{\eta_m} + \frac{2i}{\eta_m \Xi_{1m}} \sum_{n=0}^{\infty} \{B_n + C_n\} \, sin(s_n L) s_n Q_{mn} \tag{4.24}$$

or

$$H_m^+ = \frac{F_0 \delta_{0m}}{\eta_m} + \frac{2i}{\eta_m \Xi_{1m}} \sum_{n=0}^{\infty} L_m^+ sin(s_n L) s_n Q_{mn}, \tag{4.25}$$

where

$$H_m^+ = A_m + D_m$$

and

$$L_m^+ = B_m + C_m.$$

Similarly by subtracting (4.23) from (4.20) we get

$$A_m - D_m = \frac{F_0 \delta_{0m}}{\eta_m} - \frac{2i}{\eta_m \Xi_{1m}} \sum_{n=0}^{\infty} \{B_n - C_n\} \, cos(s_n L) s_n Q_{mn} \tag{4.26}$$

or

$$H_m^- = \frac{F_0 \delta_{0m}}{\eta_m} - \frac{2}{\eta_m \Xi_{1m}} \sum_{n=0}^{\infty} L_m^- cos(s_n L) s_n Q_{mn}, \tag{4.27}$$

where

$$H_m^- = A_m - D_m$$

and

$$L_m^- = B_m - C_m.$$

The pressures across the regions at interfaces are continuous, that are

$$\psi_2(r, -L) = \begin{cases} \psi_1(r, -L), & 0 \le r \le h \\ i\beta^{-1} \frac{\partial \psi_2}{\partial z}(r, -L), & h \le r \le b \end{cases} \tag{4.28}$$

and

$$\psi_2(r,L)=\begin{cases}\psi_3(r,L), & 0\le r\le h\\ -i\beta^{-1}\frac{\partial\psi_2}{\partial z}(r,L), & h\le r\le b\end{cases}. \tag{4.29}$$

By substituting (4.9) and (4.10 into (4.28) we found,

$$\sum_{n=0}^{\infty}\left\{B_ne^{-is_nL}+C_ne^{is_nL}\right\}R_{2n}(r)=\begin{cases}F_0R_{10}+\sum_{n=0}^{\infty}A_nR_{1n}(r), & 0\le r\le h\\ -\beta_1^{-1}\sum_{n=0}^{\infty}\left\{B_ne^{-is_nL}-C_ne^{is_nL}\right\}s_nR_{2n}(r), & h\le r\le b.\end{cases} \tag{4.30}$$

On multiplying the above expression by $rR_{2m}(r)$ and integrate over $0\le r\le b$ we have

$$\left\{B_me^{-is_mL}+C_me^{is_mL}\right\}\int_0^b R_{2m}(r)R_{2n}(r)rdr=F_0\int_0^h R_{2m}(r)R_{10}(r)rdr$$

$$+\sum_{n=0}^{\infty}A_n\int_0^h R_{2m}R_{1n}rdr-\beta_1^{-1}\sum_{n=0}^{\infty}\left\{B_ne^{-is_nL}-C_ne^{is_nL}\right\}s_n\int_h^b R_{2n}(r)R_{2m}(r)rdr. \tag{4.31}$$

On using the orthogonality relation (4.15) and then simplifying we get

$$\left\{B_me^{-is_mL}+C_me^{is_mL}\right\}\Xi_{2m}=F_0Q_{0m}+\sum_{n=0}^{\infty}A_nQ_{nm}$$

$$-\beta_1^{-1}\sum_{n=0}^{\infty}\left\{B_ne^{-is_nL}-C_ne^{is_nL}\right\}P_{nm}, \tag{4.32}$$

where

$$P_{nm}=\int_h^b R_{2n}(r)R_{2m}(r)rdr. \tag{4.33}$$

By substituting (4.10) and (4.11) into (4.29) we obtain

$$\left\{B_m e^{is_m L} + C_m e^{-is_m L}\right\} R_{2n}(r) = \begin{cases} \sum_{n=0}^{\infty} D_n R_{1n}(r), & 0 \le r \le h \\ \beta_1^{-1} \sum_{n=0}^{\infty} \left\{B_n e^{is_n L} - C_n e^{-is_n L}\right\} s_n R_{1n}(r), & \\ & h \le r \le b \end{cases} \tag{4.34}$$

On multiplying the above expression by $rR_{2m}(r)$ and integrating with respect to r over $0 \le r \le b$ we get

$$\left\{B_m e^{is_m L} + C_m e^{-is_m L}\right\} \int_0^b R_{2n}(r) R_{2m}(r) r dr = \sum_{n=0}^{\infty} D_n \int_0^h R_{1n}(r) R_{2m}(r) r dr$$

$$+ \beta_1^{-1} \sum_{n=0}^{\infty} \left\{B_n e^{is_n L} - C_n e^{-is_n L}\right\} s_n \int_h^b R_{2n}(r) R_{2m}(r) r dr. \tag{4.35}$$

On using orthogonality relation (4.15) and then simplifying the resulting equations, we found

$$\left\{B_m e^{is_m L} + C_m e^{-is_m L}\right\} \Xi_{2m} = \sum_{n=0}^{\infty} D_n Q_{nm}$$

$$+ \beta_1^{-1} \sum_{n=0}^{\infty} \left\{B_n e^{is_n L} - C_n e^{-is_n L}\right\} s_n P_{nm}. \tag{4.36}$$

By adding equations (4.32) and (4.36) we get

$$B_m + C_m = \frac{1}{2cos(s_m L)\Xi_{2m}} \left\{F_0 Q_{0m} + \sum_{n=0}^{\infty} \{A_n + D_n\} Q_{nm}\right\}$$

$$+ \frac{i\beta_1^{-1}}{cos(s_m L)\Xi_{2m}} \sum_{n=0}^{\infty} \{B_n + C_n\} sin(s_n L) s_n P_{nm}, \tag{4.37}$$

or

$$L_m^+ = \frac{F_0 Q_{0m}}{2cos(s_m L)\Xi_{2m}} + \frac{1}{2cos(s_m L)\Xi_{2m}} \sum_{n=0}^{\infty} H_n^+ Q_{nm}$$

$$+ \frac{\beta_1^{-1} i}{cos(s_m L)\Xi_{2m}} \sum_{n=0}^{\infty} L_n^+ sin(s_n L) s_n P_{nm}. \tag{4.38}$$

On subtracting equation (4.32) from (4.36) we found

$$B_m - C_m = -\frac{1}{2isin(s_mL)\Xi_{2m}}\left\{F_0Q_{0m} + \sum_{n=0}^{\infty}\{A_n - D_n\}Q_{nm}\right\}$$

$$+\frac{\beta_1^{-1}}{isin(s_mL)\Xi_{2m}}\}\sum_{n=0}^{\infty}\{B_n - C_n\}cos(s_nL)s_nP_{nm}, \tag{4.39}$$

or

$$L_m^- = \frac{iF_0Q_{0m}}{2sin(s_mL)\Xi_{2m}} + \frac{i}{2sin(s_mL)\Xi_{2m}}\sum_{n=0}^{\infty}H_n^-Q_{nm}$$

$$-\frac{i\beta_1^{-1}}{sin(s_mL)\Xi_{2m}}\sum_{n=0}^{\infty}L_n^-cos(s_nL)s_nP_{nm}. \tag{4.40}$$

In this way we obtain two systems of equations defined by (4.25) and (4.38) and (4.27) and (4.40), respectively. These systems can be solved separately to get the values of $H^{\pm}$ and $L^{\pm}$. Then unknown amplitudes $\{A_m, B_m, C_m, D_m\}$ are found from $H^{\pm}$ and $L^{\pm}$ as

- $A_m = \frac{H_m^+ + H_m^-}{2}$
- $D_m = \frac{H_m^+ - H_m^-}{2}$
- $B_m = \frac{L_m^+ + L_m^-}{2}$
- $C_m = \frac{L_m^+ - L_m^-}{2}$

In the next section, the systems defined in this section are truncated and then are solved numerically.

4.2 Numerical Results

Here the system of equations (4.38) and (4.40) are truncated upto N terms and are solved numerically. The computations are performed in Mathematica. For

computation, the physical dimensional heights are fixed as: $\overline{h} = 0.1m$, $\overline{a} = 0.2m$, and $\overline{b} = 0.28m$ for cavity involving case, and $\overline{h} = 0.1m$, $\overline{a} = 0.2m = \overline{b}$, for the case without cavity inclusion. The half length of the chamber is fixed as $L = 0.1m$. The compressible fluid density $\rho = 1.2043kgm^{-3}$ and sound speed $c = 343ms^{-1}$ remain unchanged. The specific admittance $\beta^{-1} = i\zeta - \eta$, where $\zeta = 0.5$, $-1 \leq \eta \leq 3$ for fibrous sheet and $0 < \zeta < 3$, $-1 \leq \eta \leq 3$ for perforated sheet is considered. In Figs. 4.2-4.17, the pressures and normal velocities are plotted at $z = L^{\pm}$. From the graphs presented in Figs. 4.2-4.17, it can be seen that the real and imaginary parts of pressure and normal velocities match exactly as considered in matching conditions (4.16), (4.17) and (4.28) and (4.29).

Moreover, in Figs. 3.6 and 3.7 the transmission loss against frequency for fibrous and perforated types of lining is shown with and without cavity respectively. It can be seen that by changing the properties of lining the TL is changed. The variation is also evident with and without cavity inclusion.

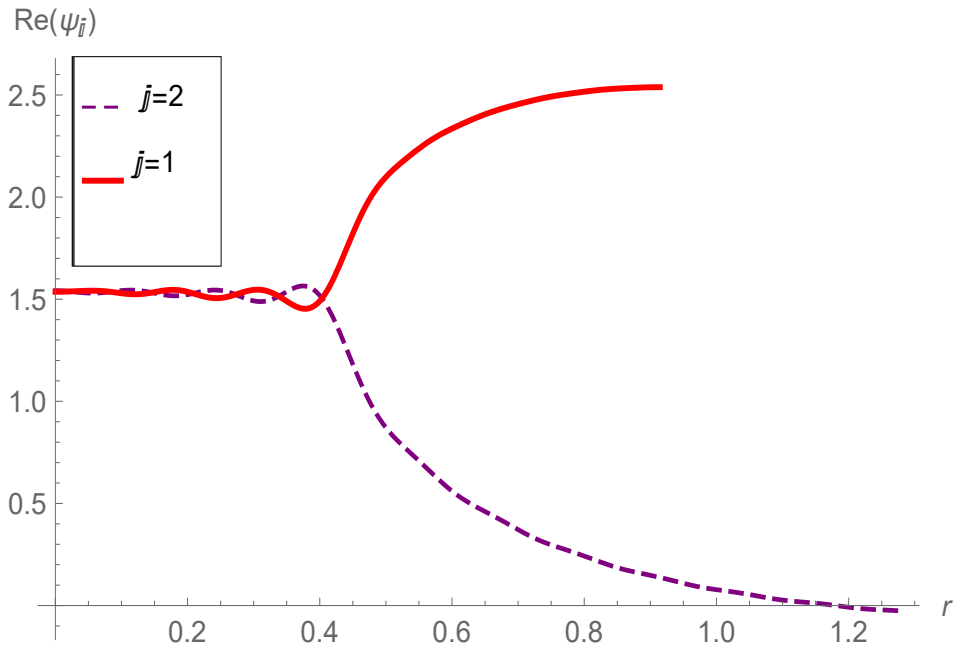

(a)

FIGURE 4.2: At $z = -L$, the real parts for pressures against radius r where $\overline{a} = 0.2m, \overline{b} = 0.28m$, $f = 250Hz$ and $N = 20$.

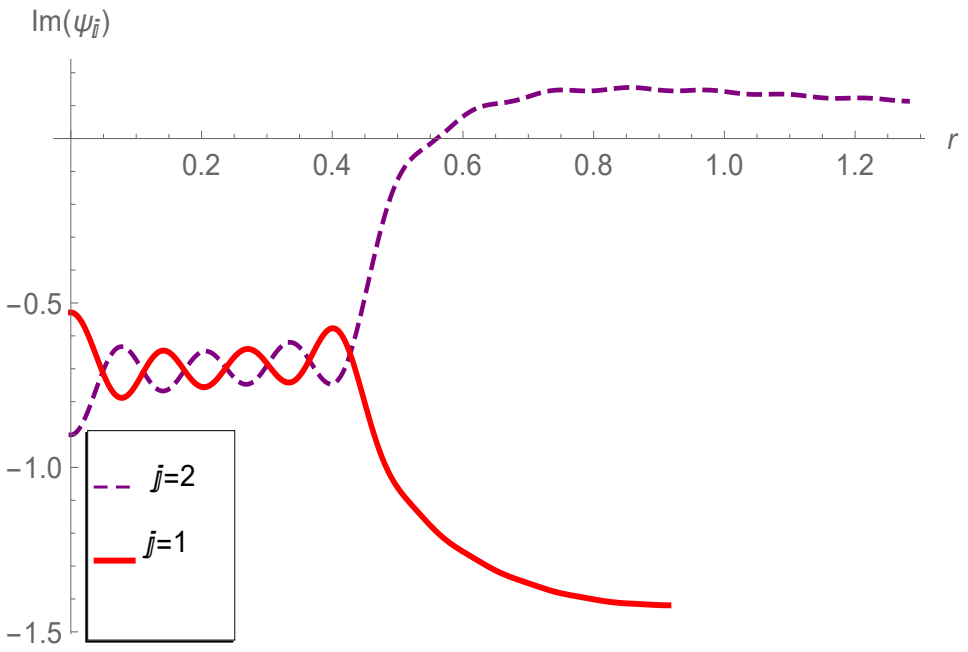

(a)

FIGURE 4.3: At $z = -L$, the imaginary parts for pressures against radius r where $\overline{a} = 0.2m, \overline{b} = 0.28m$, $f = 250Hz$ and $N = 20$.

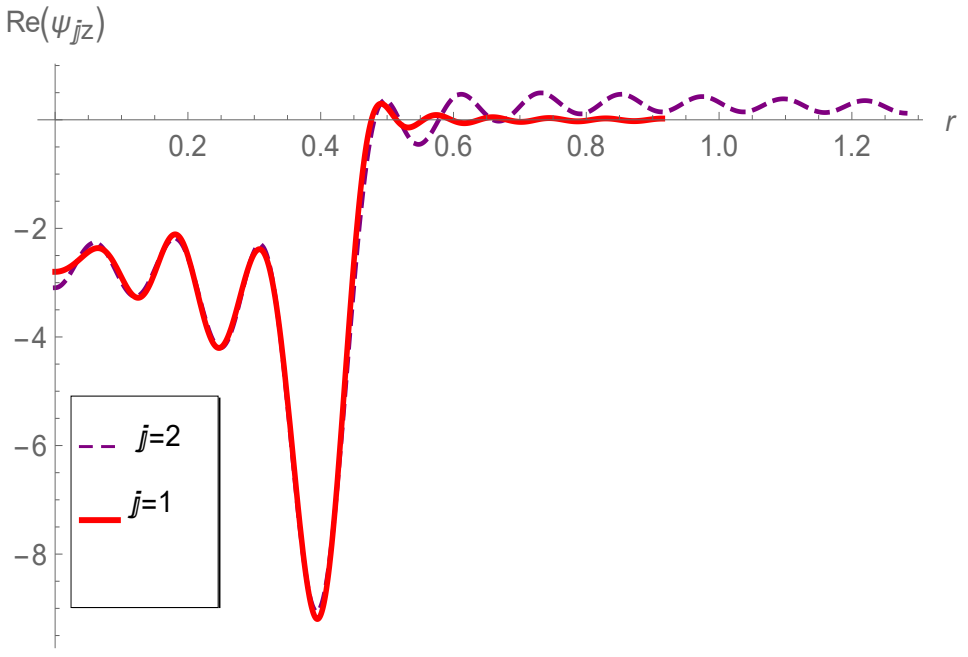

(a)

FIGURE 4.4: At $z = -L$, the real parts for normal velocities against radius r where $\overline{a} = 0.2m, \overline{b} = 0.28m$, $f = 250Hz$ and $N = 20$.

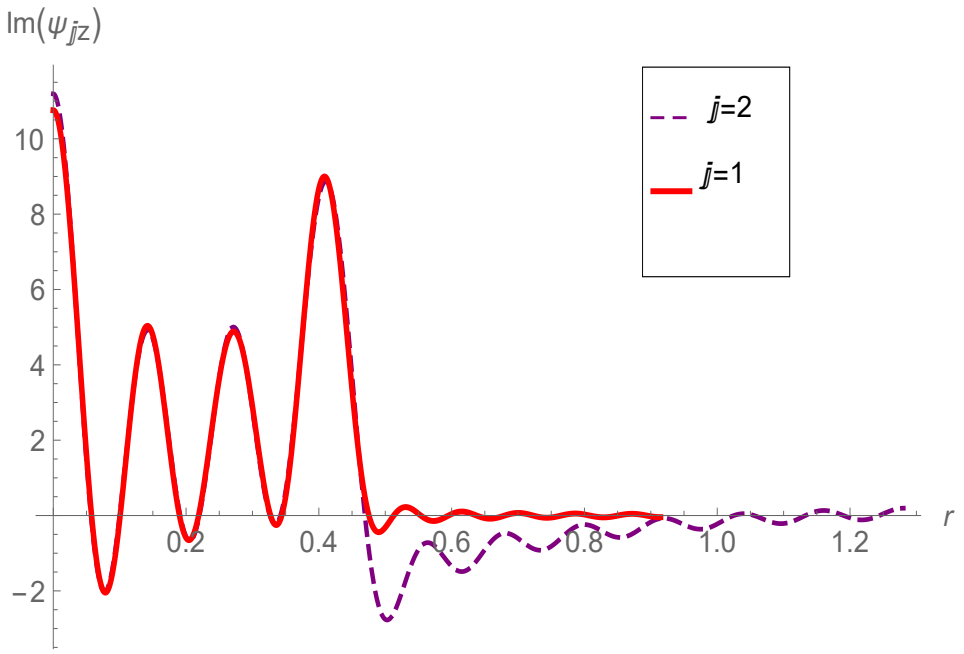

(a)

FIGURE 4.5: At $z = -L$, the imaginary parts for normal velocities against radius r where $\overline{a} = 0.2m, \overline{b} = 0.28m$, $f = 250Hz$ and $N = 20$.

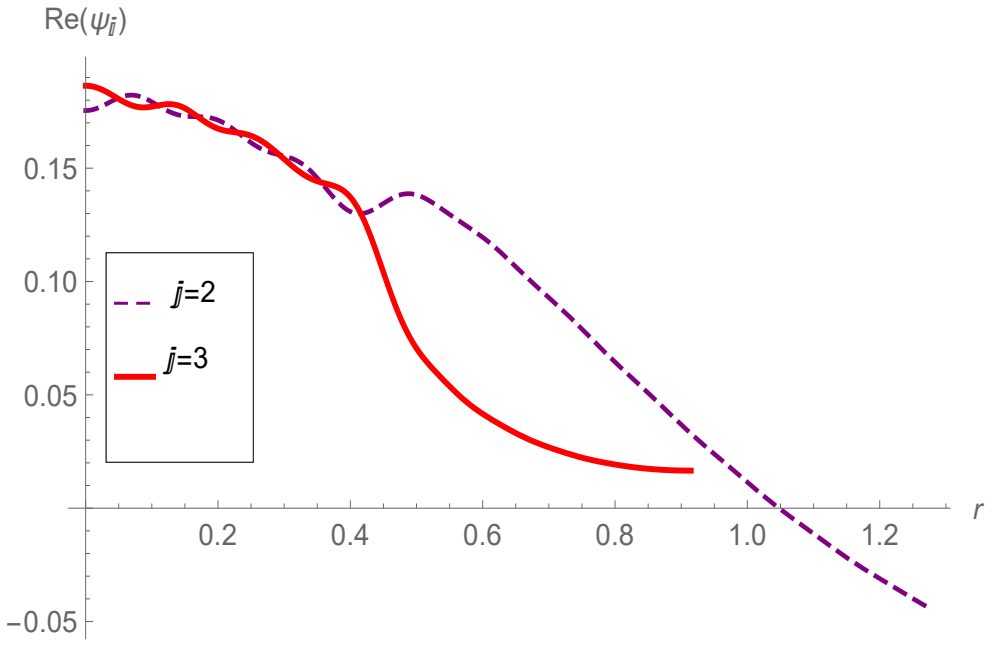

(a)

FIGURE 4.6: At $z = L$, the real parts for pressures against radius r where $\overline{a} = 0.2m, \overline{b} = 0.28m$, $f = 250Hz$ and $N = 20$.

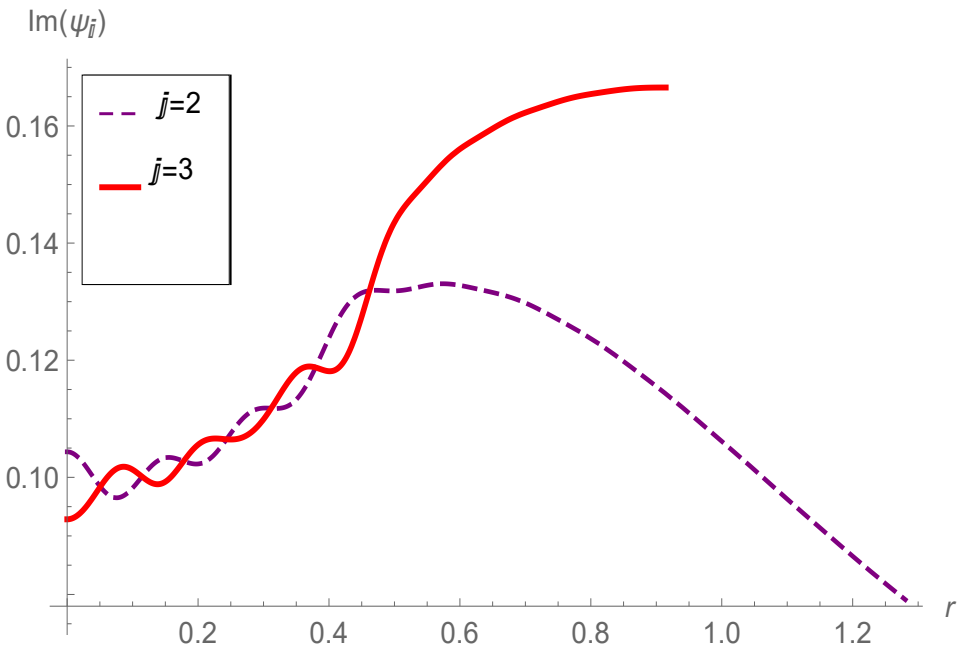

(a)

FIGURE 4.7: At $z = L$, the imaginary parts for pressures against radius r where $\overline{a} = 0.2m, \overline{b} = 0.28m$, $f = 250Hz$ and $N = 20$.

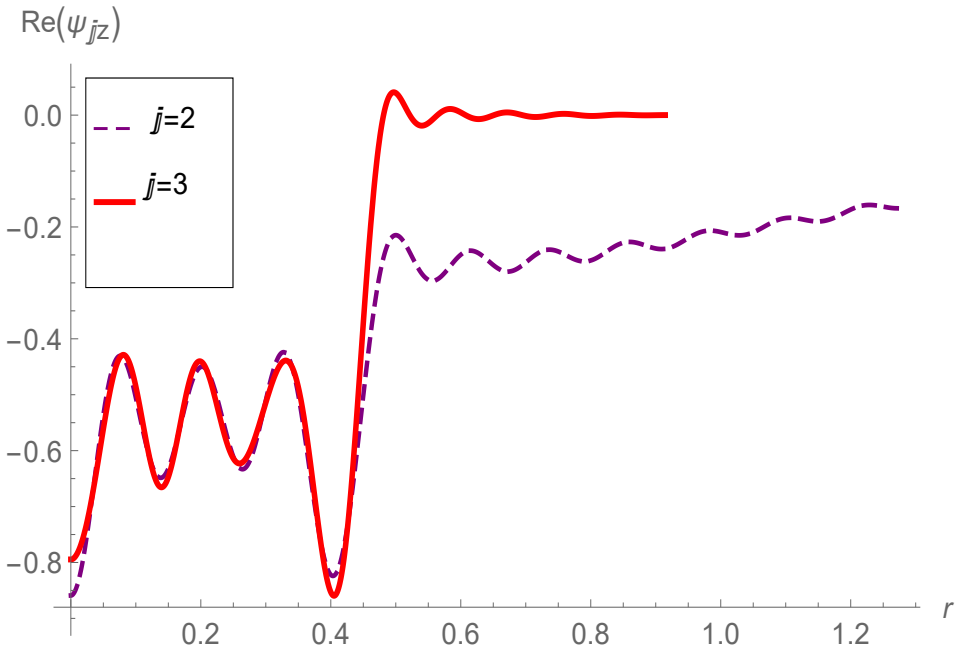

(a)

FIGURE 4.8: At $z = L$, the real parts for normal velocities against radius r where $\overline{a} = 0.2m, \overline{b} = 0.28m$, $f = 250Hz$ and $N = 20$.

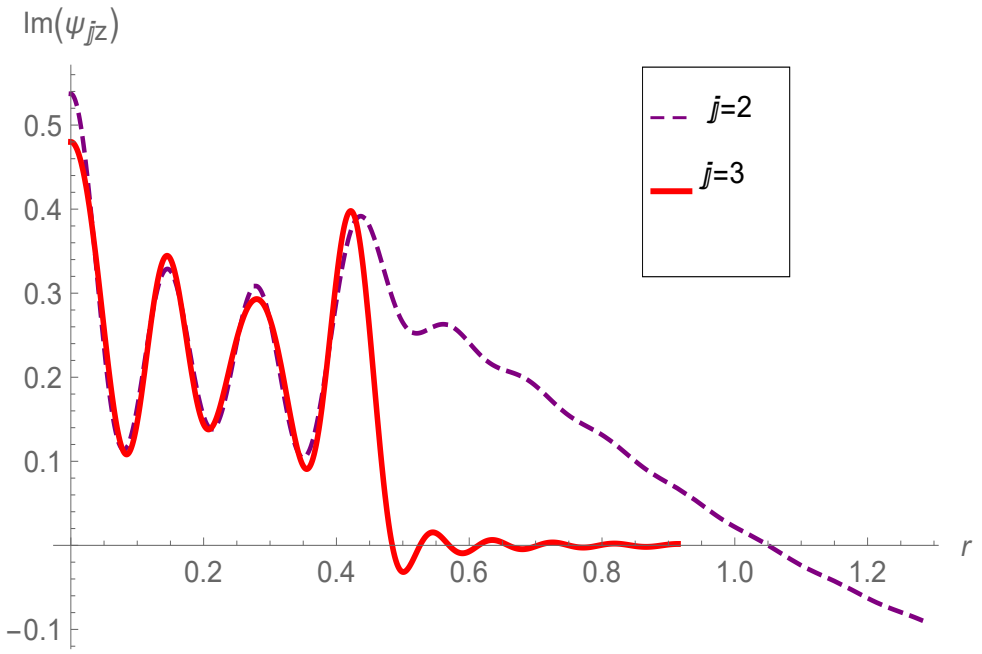

(a)

FIGURE 4.9: At $z = L$, the imaginary parts for normal velocities against radius r where $\overline{a} = 0.2m, \overline{b} = 0.28m$, $f = 250Hz$ and $N = 20$.

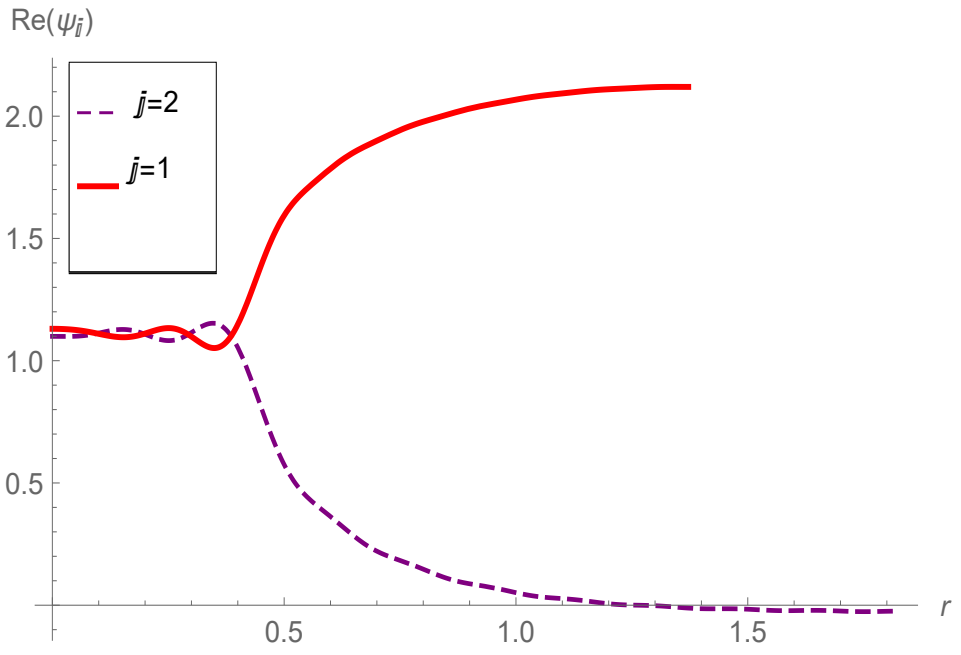

(a)

FIGURE 4.10: At $z = -L$, the real parts for pressures against radius r where $\overline{a} = 0.3m, \overline{b} = 0.4m$, $f = 250Hz$ and $N = 20$.

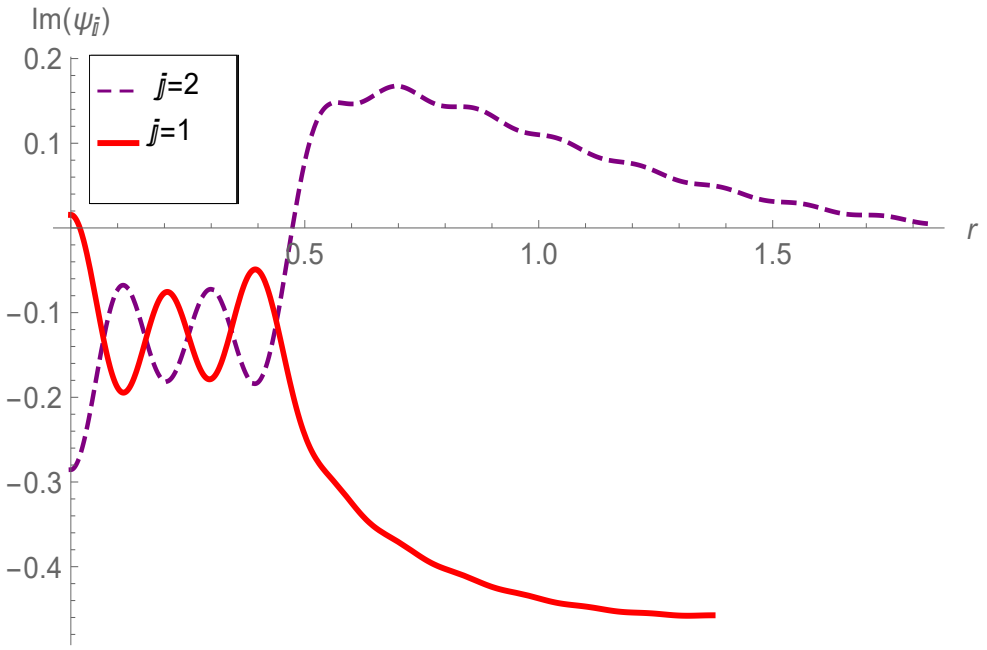

(a)

FIGURE 4.11: At $z = -L$, the imaginary parts for pressures against radius r where $\overline{a} = 0.3m, \overline{b} = 0.4m$, $f = 250Hz$ and $N = 20$.

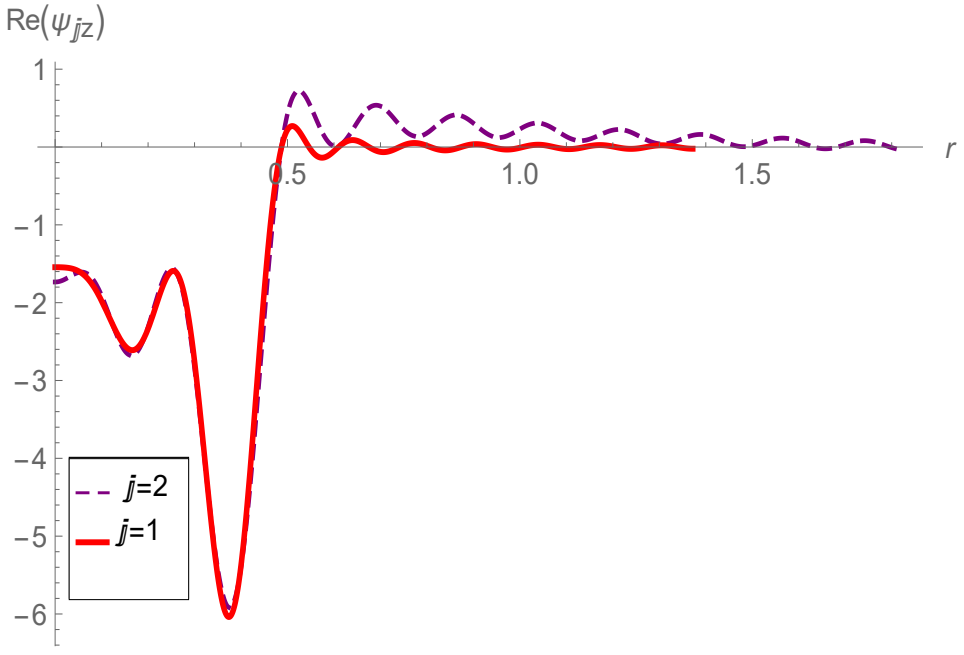

(a)

FIGURE 4.12: At $z = -L$, the real parts for normal velocities against radius r where $\overline{a} = 0.3m, \overline{b} = 0.4m$, $f = 250Hz$ and $N = 20$.

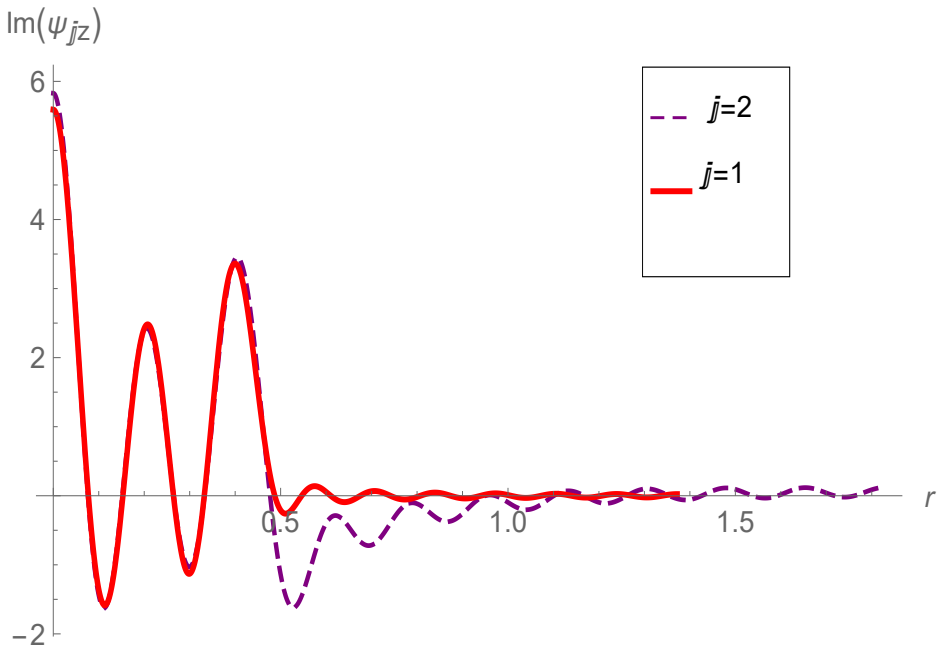

(a)

FIGURE 4.13: At $z = -L$, the imaginary parts for normal velocities against radius r where $\overline{a} = 0.3m, \overline{b} = 0.4m$, $f = 250Hz$ and $N = 20$.

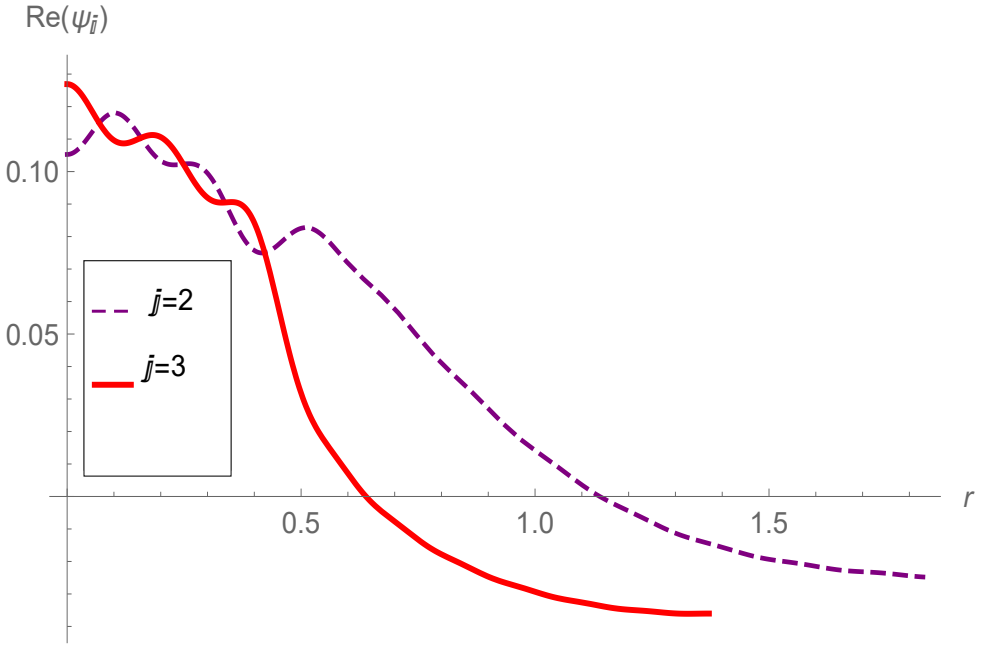

(a)

FIGURE 4.14: At $z = L$, the real parts for pressures against radius r where $\overline{a} = 0.3m, \overline{b} = 0.4m$, $f = 250Hz$ and $N = 20$.

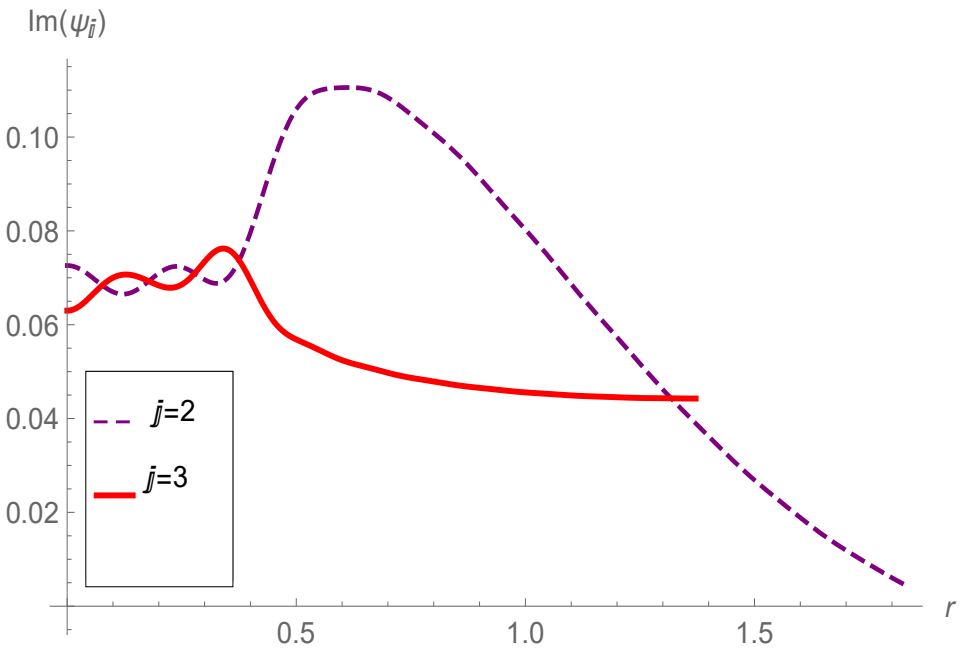

(a)

FIGURE 4.15: At $z = L$, the imaginary parts for pressures against radius r where $\overline{a} = 0.3m, \overline{b} = 0.4m$, $f = 250Hz$ and $N = 20$.

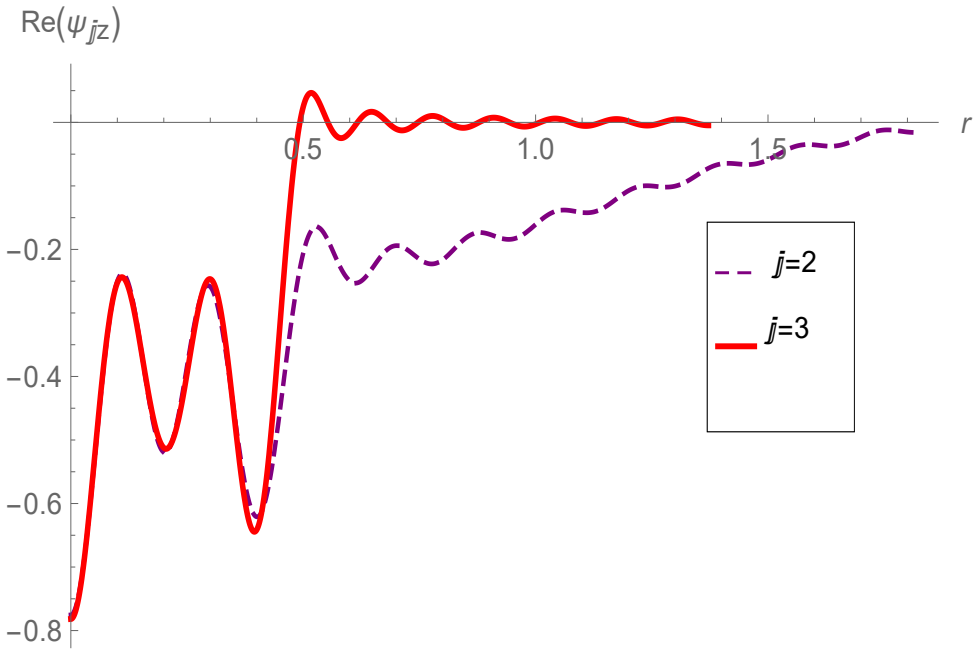

(a)

FIGURE 4.16: At $z = L$, the real parts for normal velocities against radius r where $\overline{a} = 0.3m, \overline{b} = 0.4m$, $f = 250Hz$ and $N = 20$.

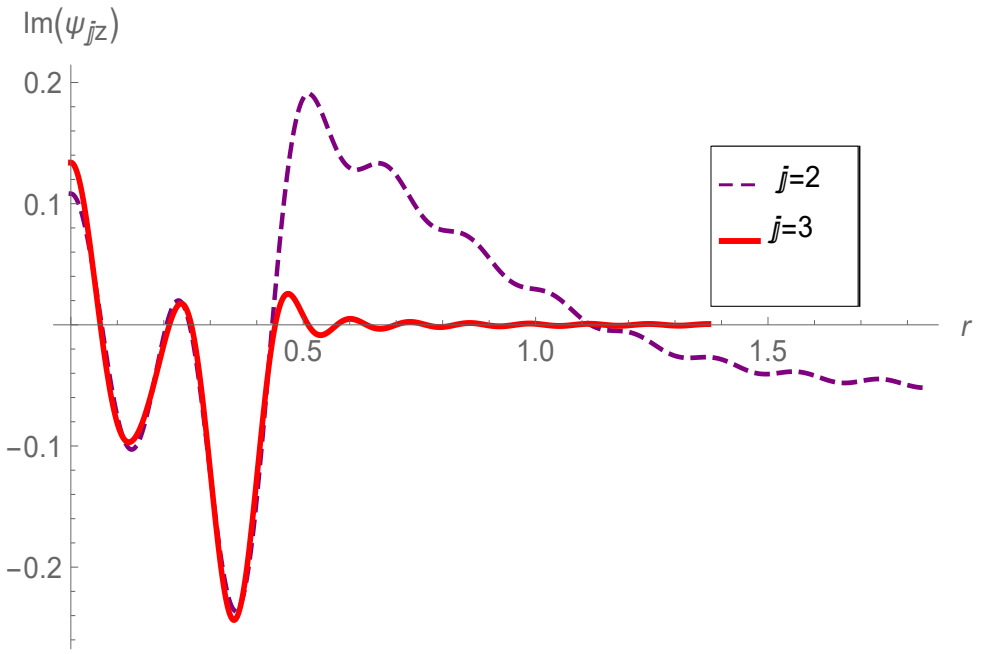

(a)

FIGURE 4.17: At $z = L$, the imaginary parts for normal velocities against radius r where $\overline{a} = 0.3m, \overline{b} = 0.4m$, $f = 250Hz$ and $N = 20$.

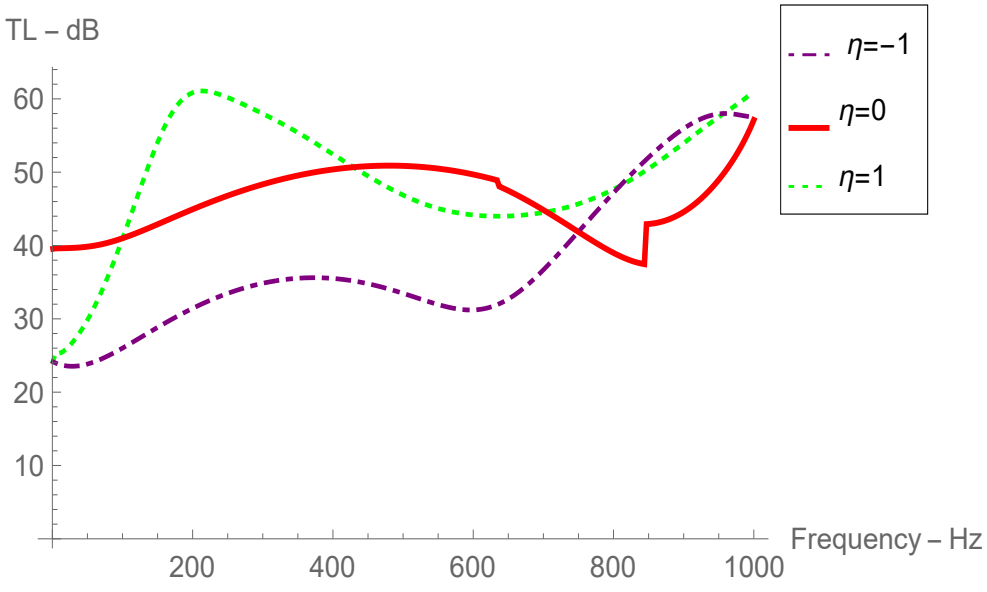

(a)

FIGURE 4.18: The transmission loss against frequency for fibrous sheet with $\overline{a} = 0.2m$, $\overline{b} = 0.28m$, and $h = 0.1m$ for $N = 20$.

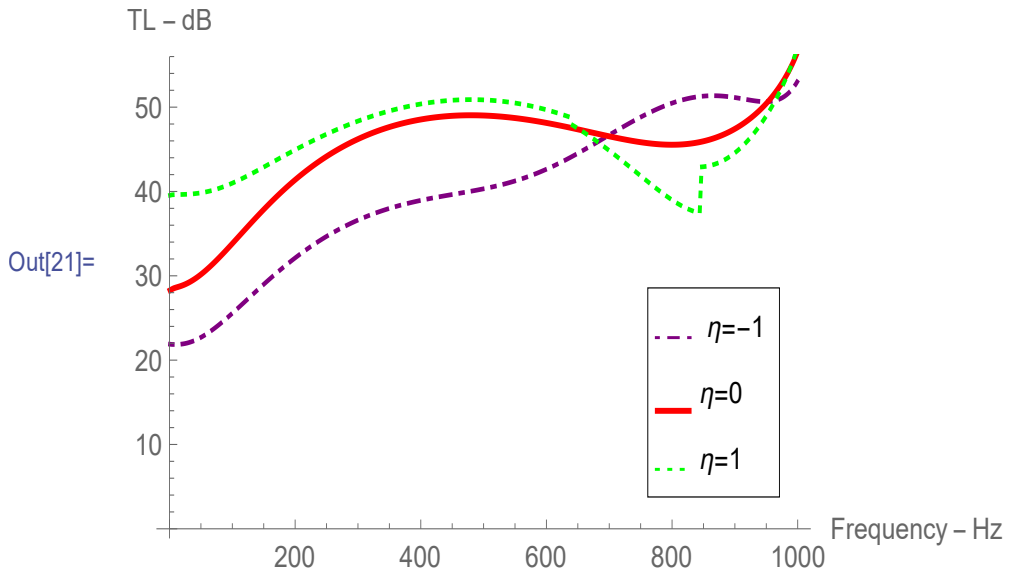

(a)

FIGURE 4.19: The transmission loss against frequency for perforated sheet with $\overline{a} = 0.2m$, $\overline{b} = 0.28m$, and $h = 0.1m$ for $N = 20$.

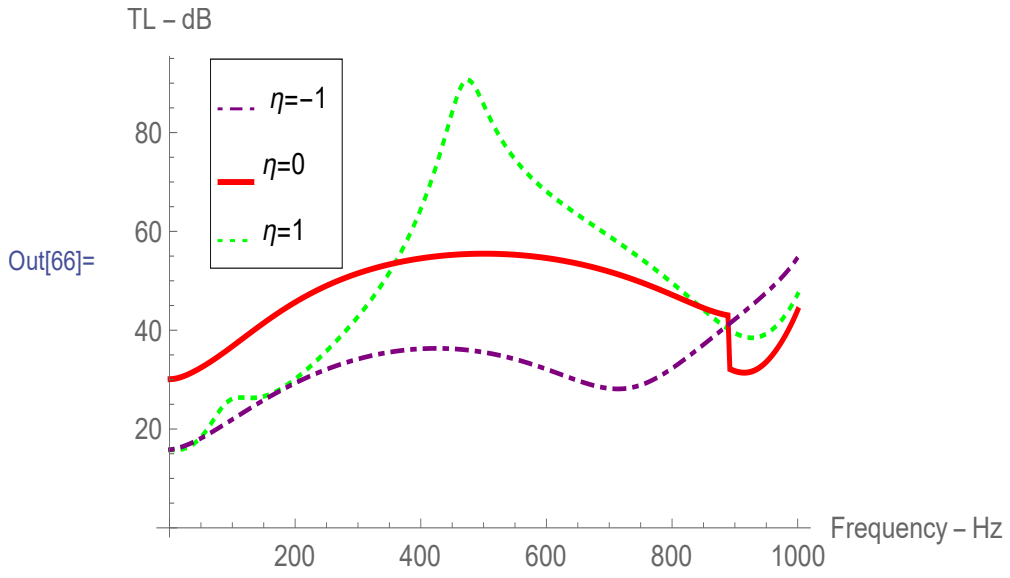

(a)

FIGURE 4.20: The transmission loss against frequency for fibrous sheet with $\overline{a} = \overline{b} = 0.2m$ and $h = 0.1m$ for $N = 20$.

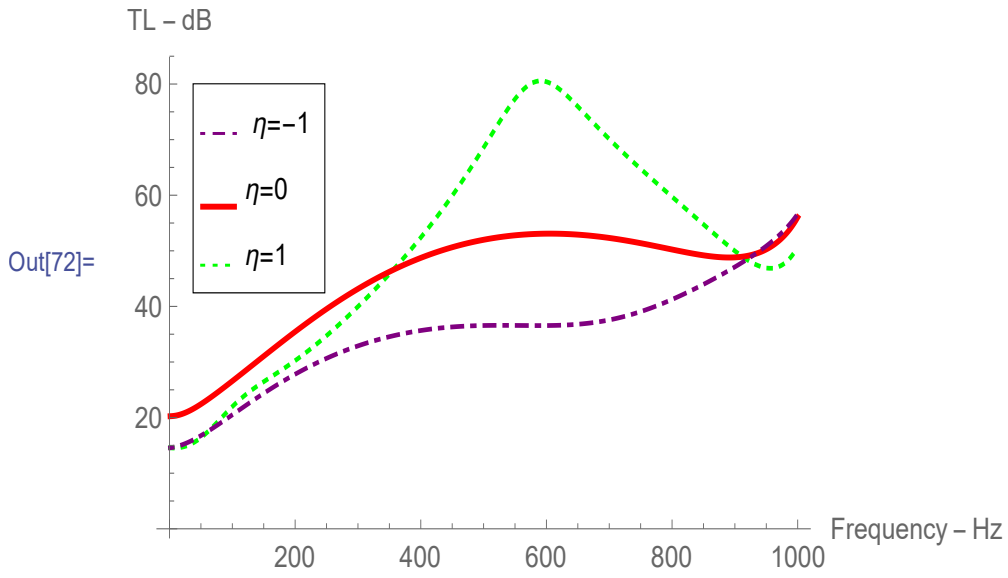

(a)

FIGURE 4.21: The transmission loss against frequency for perforated sheet with $\overline{a} = \overline{b} = 0.2m$ and $h = 0.1m$ for $N = 20$.

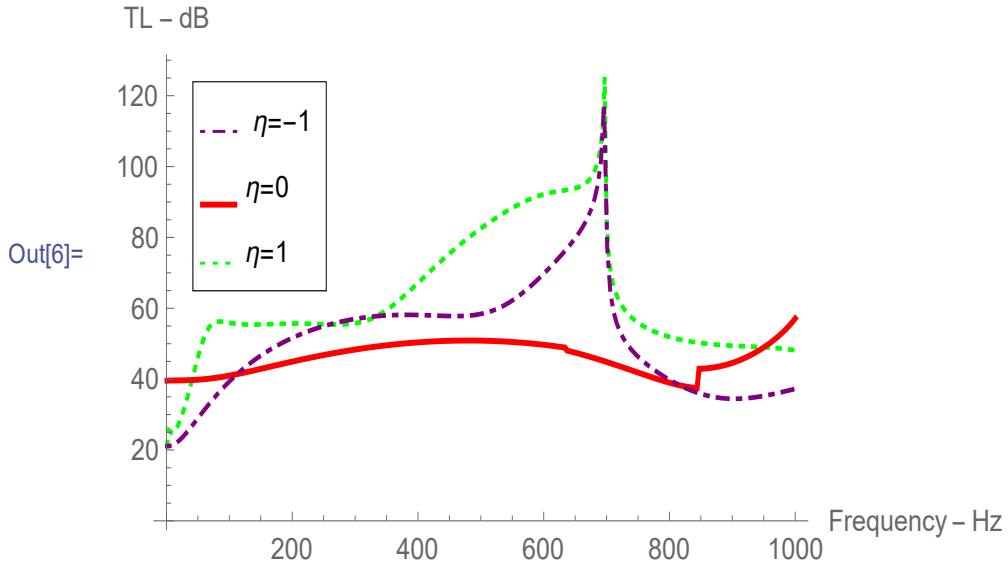

(a)

FIGURE 4.22: The transmission loss against frequency for fibrous sheet with $\overline{a} = 0.3m$, $\overline{b} = 0.4m$, and $h = 0.1m$ for $N = 20$.

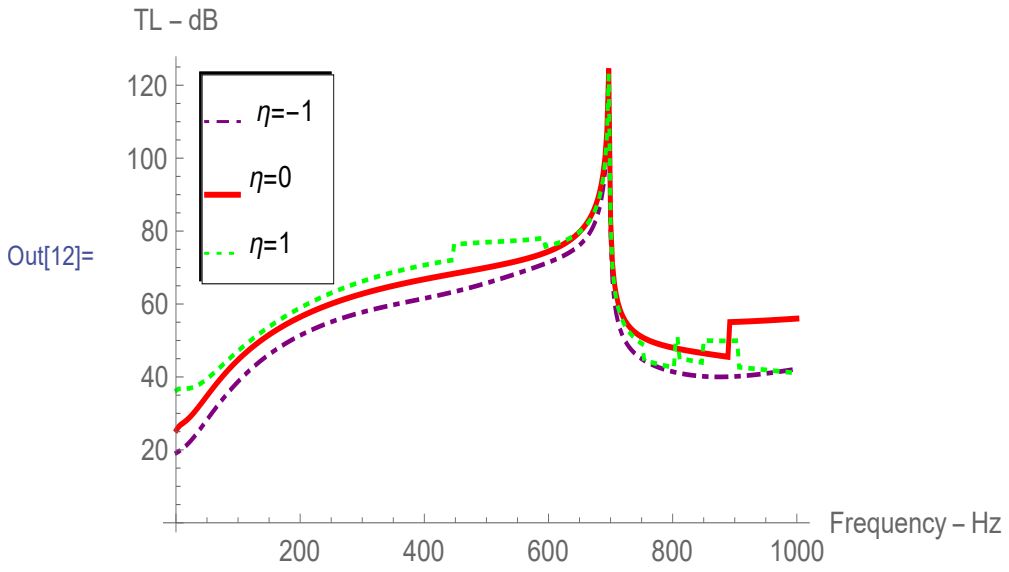

(a)

FIGURE 4.23: The transmission loss against frequency for perforated sheet with $\overline{a} = 0.3m$, $\overline{b} = 0.4m$, and $h = 0.1m$ for $N = 20$.

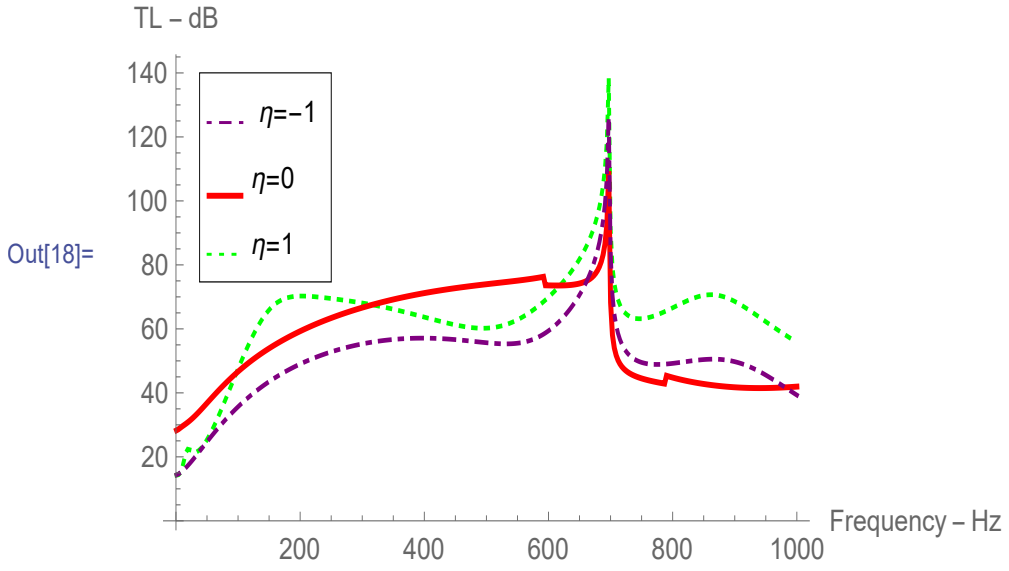

(a)

FIGURE 4.24: The transmission loss against frequency for fibrous sheet with $\overline{a} = \overline{b} = 0.3m$ and $h = 0.1m$ for $N = 20$.

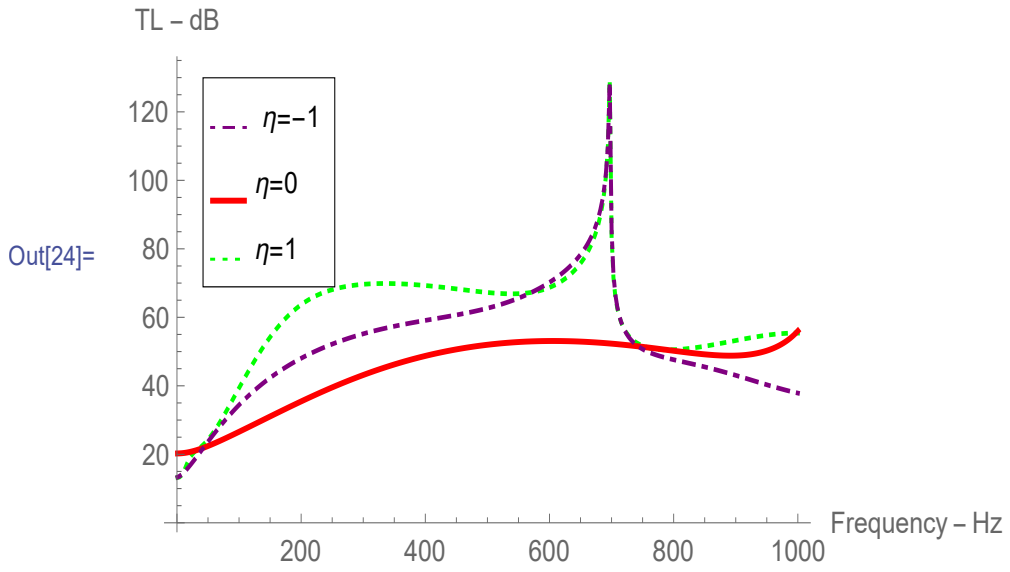

(a)

FIGURE 4.25: The transmission loss against frequency for perforated sheet with $\overline{a} = \overline{b} = 0.3m$ and $h = 0.1m$ for $N = 20$.

Chapter 5

Discussion and conclusion

The work presented in this thesis is relevant to dissipative device that can be a part of hybrid silencer. The reflection and transmission of acoustic waves in cylindrical waveguides is analyzed. The physical problems are governed by Helmholtz's equation along with the acoustic absorbing lining. The Mode-Matching (MM) technique has been used to find the solutions of these modelled problems.

In Chapter-3, two problems are discussed. First problem includes a single circular duct radiated by a plane piston. The bounding circular surface of the duct comprises a coating of absorbing material. This coating is assumed as of the perforated and fibrous material. The results show that variation in properties of absorbing material significantly affect the scattering amplitudes. Second problem comprises as cylindrical waveguides containing two duct regions of different heights. This problem involves the effect of height discontinuity on scattering. The porous lining has also been used in the region with greater radius to dissipate the acoustics waves. The results show that the height discontinuity and dissipative material both affect the reflecting and absorbing powers.

In Chapter-4, an expansion chamber with flanged inclusion at interfaces is assumed to analyze the transmission loss of hybrid silencer. The inside walls of the chamber are coated with fibrous and perforated material. The transmission loss against frequency is analyzed with respect to the geometrical configuration and properties of dissipative material. It is seen that the transmission loss is greatly effected by

the variation in geometry of the chamber and by the change in properties of the dissipative material.

Bibliography

[1] F. V. Hunt, "Origins in acoustics," *Acoustical Society of America*, 2nd edition, pp. 518-524 Woodbury, NY 1992.

[2] M. Mersenne, "An early chapter in the history of sound," *Acoustica*, vol. 2 pp. 96-99 1951.

[3] D. C. Miller, "Anecdotal history of the science of sound,"*Macmillan*, New York, opposite. p. 84 1935.

[4] M. A. Lenihan, "The velocity of sound in air,"*Acustica*, vol. 2, pp. 205-212 1952.

[5] W. C. Sabine and Reverberation, "Reprinted in collected papers on acoustics," *Penin sula publishing Los Altos* 1900.

[6] J. Ih and B. Lee, "Analysis of higher order mode effects in the circular expansion chamber with mean flow," *Acoustical Society of America*, vol. 77, pp. 1377-1388, 1985.

[7] I. D. Abrahams, "Scattering of sound by two parallel semi-infinite screens," *Wavemotion*, vol. 9, pp. 289-300, 1987.

[8] G. Bao, and W. Zhang, "An improved mode-matching method for large cavities," *IEEE Antennas and Wireless propagation letters*, vol 4, no.1, pp. 393-396, 2005.

[9] M. Hassan and A. D. Rawlins, "Radiation from a two dimensional duct," *Canadian Journal of Physic*, vol.1, pp.375-384, 1997.

[10] R. Kirby, Zahari Zlatev and Peter Mudge, "On the scattering of torsional elastic waves from axisymmetric defects in coated pipes," *Sound and vibration*, vol. 331, no.17,pp. 3989-4004, 2012.

[11] J. B. Lawrie and Idil. M. M. Guled, "On tuning a reactive silencer by varying the position of an internal membrane," *Acoustical Society of America*, vol. 120, pp. 780, 2006.

[12] B. Polat, "Analyzed the diffraction in Plane wave by a semi-infinite soft/hard parallel-plate waveguide," *Canadian Journal of Physic*, vol. 76, pp. 771-784, 1998.

[13] A. D. Rawlins, "Wave propagation in a bifurcated impedance-lined cylindrical waveguide," *Engineering Mathematics*, vol. 59, no.4, pp. 419-435, 2007.

[14] I. H. Tayyar, "Wiener-Hopf analysis of the parallel plate waveguide with opposing rectangular dielectric-filled grooves," *Canadian Journal of Physic* vol. 86, pp. 733-745, 2008.

[15] A. D. Rawlins, "Two waveguide trifurcation problems," *Mathematical Proceedings of Cambridge Philosopher Society*, vol. 121, pp. 555-573, 1997.

[16] A. Buyukaksoy and B. Polat, " A bifurcated waveguide problem," *Physical and Engineering Sciences*, vol. 51, no. 3, pp. 196-202, 1999.

[17] M. Ayub, M. H. Tiwana and A. B. Mann, "Analysis of diffraction of dominant mode in an acoustic impedance loaded trifurcated duct," *ZeitschriftfurNaturforschung*, vol. 65a: pp. 995-1008, 2010.

[18] M. Ayub, M. H. Tiwana and A. B. Man, "Acoustic diffraction in a trifurcated waveguide with mean how," *Communication inNonlinear Science and Numerical simulation*, vol. 15, pp. 3939-3949, 2010.

[19] K. S. Peat, "The acoustical impedance at the junction of an extended inlet or outlet duct," *Sound Vibration*, vol. 150, no. 1, pp. 101-110, 1991.

[20] B. Nilsson and O. Brander, "The propagation of sound in cylindrical ducts with mean flow and bulk-reacting lining. I-Modes in an infinite duct," *Ins.t Math. Appl* vol. 26, no. 3, pp. 269-298, 1980.

[21] J. W. Miles, "The analysis of plane discontinuities in cylindrical tubes. Part I," *The Acoustical Society of America*, vol. 17,no. 3, pp. 259-271, 1946.

[22] R. Nawaz, M. Afzal and M. Ayub, "Acoustics propagation in two dimensional waveguide for membrane bounded duct," *Communication in Nonlinear Science and Numerical Simulation* ,vol. 20, no. 2, pp. 421-433, 2015.

[23] R. Nawaz and J. B. Lawrie, "Scattering of fluid-structure coupled wave at a flanged junction between two flexible wave guide," *Acoustical Society of America*, vol. 134 no. 2, pp. 421-433, 2013.

[24] A. Damir and A. Buyukaksoy, "Transmission of sound wave in a cylindrical duct with an acoustically lined muffler," *Engineering Science* ,vol. 41, pp. 2411-2427, 2003.

[25] M. Afzal, R. Nawaz, M. Ayub and Abdul Wahab, "Acoustic scattering in flexible waveguide involving step discontinuity," *PloS one* vol. 9, no. 8, pp. e103807 2014.

[26] M Afzal, R. Nawaz and A. U. Jan, "Attenuation of dissipative device involving coupled wave scattering and change in properties," *Applied Mathematics and Computation*, vol, 290, pp. 154-163, 2016.

[27] M. Afzal, M. Ayub, R. Nawaz and Abdul "Wahab Mode-Matching solution of scattering problems in flexible waveguide with abrupt geometric changes, Journal of Imaging, Multi-scale and high contrast partial differential equations," *Mathematical Society*, vol. 660, pp. 113, 2016.

[28] J. B. Lawrie and M. Afzal, "Acoustic scattering in a waveguide with hight discontinuity bridged by a membrane a tailored Galerkin approach," *Engineering Mathematics*, vol. 105 no. 1 pp. 99-115, 2017.

[29] R. Nawaz, A. U. Jan and M. Afzal, "Fluid structure coupled wave scattering in a flexible duct at the junction of planer discontinuities," *Advances in Mechanical Engineering* vol. 9, no. 7, pp. 1-11, 2017.

[30] S. Shafique, M. Afzal and R. Nawaz, "On Mode-Matching analysis of fluid structure coupled wave scattering between two flexible waveguides," *Canadian journal of physics* vol. 95, no. 6, pp. 581-589, 2017.

[31] T. Nawaz, M. Afzal and R. Nawaz, "The scattering analysis of trifurcated waveguide involving structural discontinuities," *Advances in Mechanical Engineering*,, vol. 11, no. 7, pp. 1-11, 2019.

[32] J. U. Satti, M. Afzal and R. Nawaz, "Scattering analysis of a partitioned wave-bearing cavity containing different material properties," *Physica Scripta*, vol. 94 https://doi.org/10.1088/1402-4896/ab2ab1 (2019).

[33] T. D. Rossing, "Handbook of acoustics, Springer," 2007.

[34] L. E. Kinsler, A. R. Frey, A. B. Coppens and J. V. Sanders, Hand book, "Fundamental of acoustics," 4th Edition, Wiley, 1999.

[35] D. Rawlins, "Radiation of sound from an unchanged rigid cylinderical duct with an acoustically absorbing internal surface," *Proceedings of the Royal Society of London*, Series A, Mathematical and Physical Sciences , vol. 361, pp. 65-91, 1978.

[36] R. M. Pullen and J.B. Lawrie, "Reflection and transmission at the junction between two sections of circular cylindrical shell," *ICSV*21 *Beijing China*, vol. 213, pp. 1-7, 2014.

[37] R. M. Pullen, "Acoustic scattering in circular cylindrical shells: A model approach based on a generalized orthogonality relation. PhD thesis," Brunel University 2017.

[38] Morse and U. Ingard, Hand book, "Theoretical acoustics," *Publisher* : *Princeton University*, Press, 1986.

[39] M. Abramowitz and I. A. Stegun "Handbook of Mathematical Functions",*Dover Publications*, 9th Edition, 1964.

[40] G. Stokes, "On the theories of the internal friction of fluids in motion and of the equilibrium and motion of elastic solids," *Transactions of the Cambridge Philosophical Society*, vol. 8, pp. 75-102, (1845).